galaxies

MDPI

Review

What Drives the Ionized Gas Outflows in Radio-Quiet AGN?

Mainak Singha [1,2,3,4,*], Christopher P. O'Dea [1] and Stefi A. Baum [1]

[1] Department of Physics & Astronomy, University of Manitoba, 30A Sifton Road, Winnipeg, MB R3T 2N2, Canada
[2] Astrophysics Science Division, NASA Goddard Space Flight Center, Greenbelt, MD 20771, USA
[3] Southeastern Universities Research Association, 1201 New York Ave. NW, Suite 430, Washington, DC 20005, USA
[4] Center for Research and Exploration in Space Science and Technology, NASA Goddard Space Flight Center, Greenbelt, MD 20771, USA
* Correspondence: singham4@myumanitoba.ca; Tel.: +1-204-474-9817

Abstract: We review the mechanisms driving the ionized gas outflows in radio-quiet (RQ) AGN. Although it constitutes ∼90% of the AGN population, what drives these outflows in these AGNs remains an open question. High-resolution imaging and integral field unit (IFU) observation is key to spatially resolving these outflows, whereas radio observations are important to comprehend the underlying radiative processes. Radio interferometric observations have detected linear, collimated structures on the hundreds of pc scale in RQ AGN, which may be very similar to the extended radio jets in powerful galaxies. Proper motions measured in some objects are sub-relativistic. Other processes, such as synchrotron radiation from shock-accelerated gas around the outflows could give rise to radio emissions as well. Near the launching region, these outflows may be driven by the thermal energy of the accretion disk and exhibit free–free emission. IFU observations on the other hand have detected evidence of both winds and jets and the outflows driven by them in radio-quiet AGN. Some examples include nearby AGN such as Mrk 1044 and HE 1353-1917. An IFU study of nearby ($z < 0.06$) RQ AGN has found that these outflows may be related to their radio properties on <100 pc scale, rather than their accretion properties. Recent JWST observations of RQ AGN XID 2028 have revealed that radio jets and wind could inflate bubbles, create cavities, and trigger star formation. Future high-resolution multi-wavelength observations and numerical simulations taking account of both jets and winds are hence essential to understand the complex interaction between radio-quiet AGN and the host from sub-pc to kpc scales.

Keywords: active galactic nuclei; black hole feedback; radio observations; jets

Citation: Singha, M.; O'Dea, C.P.; Baum, S.A. What Drives the Ionized Gas Outflows in Radio-Quiet AGN? *Galaxies* **2023**, *11*, 85. https://doi.org/10.3390/galaxies11040085

Academic Editor: Alok Chandra Gupta

Received: 17 May 2023
Revised: 30 June 2023
Accepted: 3 July 2023
Published: 12 July 2023

1. Introduction

1.1. The Need for AGN Feedback

Over the last roughly 2 decades, the enormous amount of energy released from Active Galactic Nuclei (AGN) and their coupling with the host galaxies (AGN feedback) have become key areas of study. For reviews of AGN feedback, see (e.g., [1–7]). There are three phenomena that seem to require AGN Feedback. AGN Feedback is thought to play a critical role in (1) establishing the relationship between the mass of the central supermassive black hole (SMBH) and the mass of the host galaxy (stellar velocity dispersion or luminosity) (e.g., [8–12]), (2) explaining the bright end cutoff in the luminosity function of galaxies (e.g., [13–15]), and (3) the balance of heating and cooling in the ICM of cool-core clusters (e.g., [3,4,16–18]). Because AGNs produce photons, winds, and jets, the feedback comes in two forms—radiative and kinetic. Several successful theoretical models of galaxy formation and evolution require AGN to (i) drive galactic-scale outflows that expel gas from the host galaxies reservoir [19,20], (ii) launch relativistic jets that keep the cool core of clusters of galaxies from overcooling [4,18,21].

Outflows that are apparently AGN-driven have been detected across all wavelengths, from X-ray to radio wavelengths, where the velocities of these outflows are ∼100–100,000 km s^{-1}. The outflows with the highest velocities are called ultra-fast outflows or UFO [22–24]. These UFOs are usually manifested as K-shell absorption lines and are detected in X-rays. The fast outflows emitting UV radiation reach velocities up to 10,000 km s^{-1} [25–27], which are detected in the ultra-violet (UV) with the Cosmic Origin Spectrograph on the Hubble Space Telescope (HST/COS). Warm, ionized outflows have been detected through the [O III] emission lines in the visible wavelength range through 1D and integral field unit (IFU) spectroscopy (e.g., [28–30]). There are outflows of molecular gas with velocities of hundreds to thousands of km s^{-1} seen in mm and sub-mm lines (e.g., [31–34]).

However, the powering mechanism of these outflows is a highly debated topic and an ongoing area of research. In radio-loud (RL) AGN, there is evidence for the ionized gas outflows to be driven both by the radio jets [35–37], and also by the AGN radiation field (e.g., [20,38]). Similarly, there is evidence for ionized gas outflows in RQ AGN to be driven both by radio sources (e.g., [39,40]) and by the AGN radiation field (e.g., [41–44]). The acceleration mechanism of these outflows in Radio Quiet (RQ) AGN remains unclear and complex. The observational studies of ionized gas outflows have been interpreted in several different ways, i.e., (i) radiatively driven winds from the accretion disk [41,45,46], (ii) radiation pressure from the accretion disk photons [47,48], and (iii) compact radio jets [49,50].

1.2. What Is the Difference between Radio-Loud and Radio-Quiet AGN?

Kellermann et al. [51] noticed that AGN seems to belong to two different populations of radio sources. Kellermann et al. [51] used the radio loudness parameter (R), which is defined as $R = f(4400)/f(5\ \mathrm{GHz})$, where $f(4400)$ is the optical flux from the accretion disk at 4400 Å and $f(5\ \mathrm{GHz})$ is the radio flux density at 5 GHz to distinguish between RL and RQ AGN. Kellermann et al. [51] suggested that the RL and RQ AGN boundary occurs at $R = 10$. Radio luminosity and radio source size can also be used to separate the two radio source populations [52]. The RQ AGN are fainter and smaller with radio luminosities at 6 cm $10^{21} < L_6 < 10^{23.2}$ W Hz^{-1} and radio sizes < 10 kpc, while the RL AGN are brighter and larger with $L_6 > 10^{23.2}$ W Hz^{-1} and sizes > 10 kpc [53]. The limits on radio luminosity allow Type 2 AGN (where the view to the accretion disk is blocked) to be classified as RQ/RL. Note, these are general trends with some exceptions. In particular, there is a population of powerful, compact radio sources with sizes < 10 kpc (e.g., [54]).

Evidence has been accumulating that the radio sources in the RL AGN are powered by a relativistic jet (e.g., [55,56]); while a relativistic jet is lacking in the RQ AGN (e.g., [57–59]). Of course, absence of evidence is not evidence of absence. See Padovani [60] for a helpful discussion of this issue. The question of why a minority (∼10%) of AGN are able to launch relativistic jets is beyond the scope of this review. However, even if RQ AGN does not launch relativistic jets, there is evidence for non-relativistic jets in some RQ AGN (see Section 2 below).

We expect low-power, non-relativistic jets to interact with their environments much differently than high power, relativistic jets (e.g., [61–63]). Thus, the effects of radio jet feedback need to be considered separately in RL and RQ AGN. The RQ AGN are about 90% of the AGN population; thus, it is important that we understand how AGN Feedback occurs in this dominant population. In this review we consider the effects of radiation, winds, and non-relativistic jets on the host galaxies of RQ AGN.

1.3. Outline of the Review

This paper is organized as follows: in Section 1. We briefly discuss the observational evidence of non-relativistic radio jets in RQ AGN; Section 2 focuses on the jet-driven outflows. In Section 3, we review the radio emission from AGN winds and their role in driving the outflows. Section 4 highlights a systematic IFU study to characterize the spatial

location and its relationship to accretion properties. Finally, in Section 5, we briefly discuss the recent results from JWST observations where both jets and wind could both participate in driving the ionized gas outflows.

We adopt the standard flat ΛCDM cosmology with $H_0 = 70$ km s^{-1} Mpc^{-1}, $\Omega_m = 0.3$, and $\Omega_\Lambda = 0.7$. We assume $S_\nu \sim \nu^{-\alpha}$, where S_ν is the flux density (expressed in Jy, mJy, etc.) at a given frequency ν, and α is the spectral index.

2. Observational Evidence for Jets in RQ AGN

We note that the radio properties of RQ AGN are also discussed in this Special Issue by Kharb and Silpa [64].

2.1. Observations of Linear Radio Structures

Early VLA observations were used to classify the radio morphology of nearby RQ AGN on scales of 100 s of pc into one of five categories: linear, diffuse, ambiguous, slightly resolved, and unresolved [65]. About 30–40% of the radio sources were classified as linear [65,66]. These linear radio sources are strong candidates for jets (See Figure 1). The diffuse sources are likely to be produced by star formation [67]. Subsequent imaging with the VLA found similar results for the fraction of linear sources [68–74]. In high resolution MERLIN observations of CfA Seyferts, the fraction of linear sources was 53% [75]. It is interesting that linear radio morphologies are common but do not dominate the population. It would be interesting to determine whether the incidence of linear radio sources is higher at cosmic noon.

VLBI observations of pc-scale structure tend to find high brightness temperature compact cores $T_B > 10^8$ (e.g., [57,76–80]) and sometimes pc-scale linear radio sources (e.g., [76,78,81–85]). The high brightness temperatures and pc-scale linear radio sources support the AGN nature of the radio emission.

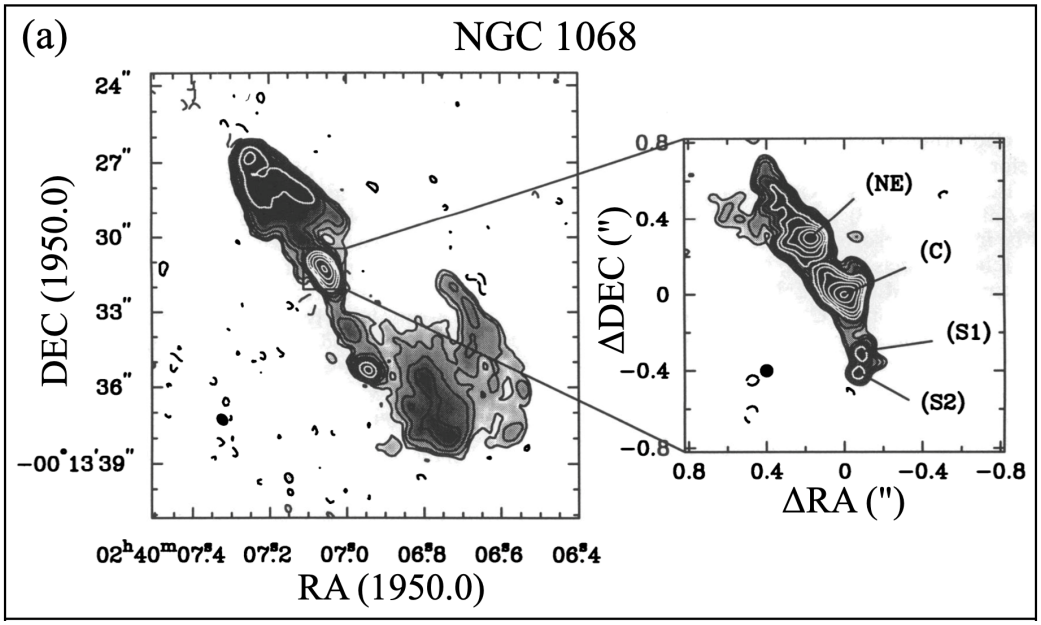

Figure 1. *Cont.*

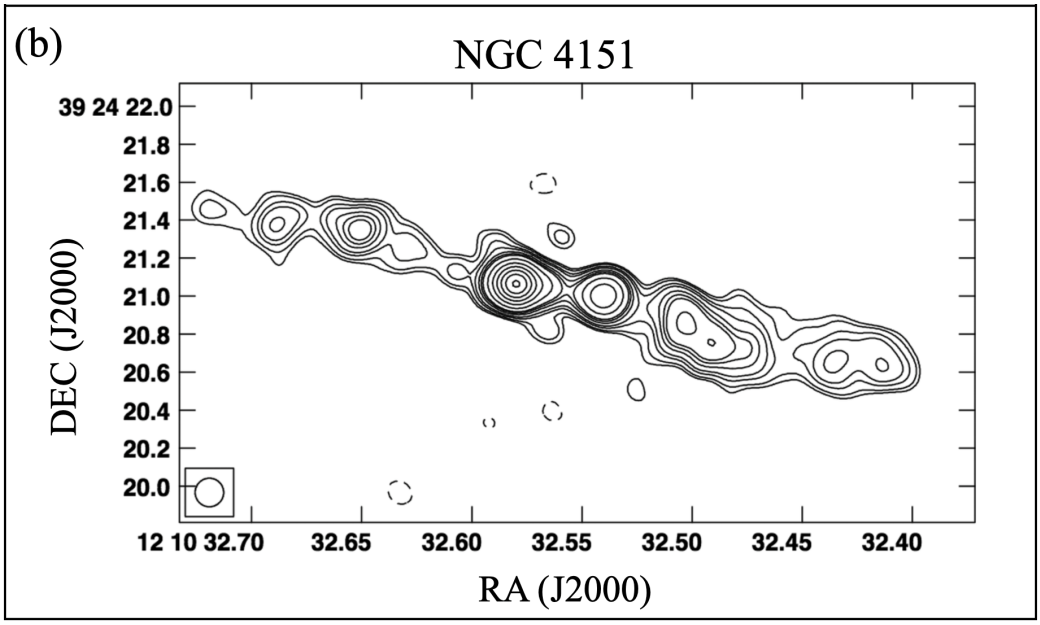

Figure 1. Observational evidence of radio jets in RQ AGN. (**a**) 6 cm continuum images of NGC 1068, taken from Gallimore et al. [86]. *Left panel:* VLA 6 cm radio continuum image of NGC 1068. The restoring beam size is $0''.49 \times 0''.38$ ($1'' \sim 100$ pc), with a position angle (PA) of 47°. *Right panel*: MERLIN 6 cm image of NGC 1068. The restoring beam is circular with a beam size of $0''.65$. The main components of the image are labeled. The bright, central ad compact component is labeled as C. The northeastern component (NE) is $\sim 0''.3$ away from C. The southern radio knots are marked as S1 and S2, which are along PA $\sim 190°$. (**b**) eMERLIN image of NGC 4151, corresponding to the central $4'' \times 2''$ ($1'' \sim 90$ pc) region, taken from Williams et al. [87]. The FWHM of the restoring beam is $0''.15 \times 0''.15$.

2.2. Evidence That the Linear Radio Structures Are Jets

Here, we discuss the evidence that the linear radio structures seen in about 50% of RQ AGN represent jets, i.e., collimated outflows of radio-emitting plasma.

1. Jet-fed radio sources are expected to propagate in a self-similar way (e.g., [88–93]). When the linear radio sources are studied in detail they sometimes resemble scaled-down versions of the jets (and sometimes lobes) in RL AGN [82,86,87] (See Figure 1). The similarity to the RL AGN suggests that the linear radio sources in RQ AGN are also jets.
2. Proper motions are observed in a few objects [57,83,94]. The apparent speed in units of c is Mrk 348 ($\beta_{\rm app} = 0.074 \pm 0.035$) and Mrk 231 ($\beta_{\rm app} = 0.14 \pm 0.052$) [57], NGC 7674 ($\beta_{\rm app} = 0.92 \pm 0.07$) [83]. NGC 3079 (initially $\beta_{\rm app} = 0.12 \pm 0.02$, but then decelerating) [94]. These proper motions confirm outflow, i.e., these are jets. The proper motions are sub-relativistic confirming that the jets are non-relativistic. *Caveat*—the proper motions may refer to some feature, e.g., a shock or the jet working surface, which does not represent the actual jet flow. There are also subluminal upper limits on proper motion—NGC 5506 ($\beta_{\rm app} = 0.21 \pm 0.17$) [83], NGC 1068 ($\beta_{\rm app} < 0.07$) [95], and NGC 4151 ($\beta_{\rm app} < 0.14$ and < 0.25 for different components) [96].

Examination of side-to-side brightness ratios [57] and comparison of the radio properties of Seyfert Is and IIs [58] argue against Doppler boosting of the radio emission. The radio morphologies and proper motions of some of the RQ AGN are thus reminiscent of another class of compact radio sources, the Compact Symmetric Objects as noted previously [57,83]. Interestingly, the proper motions seem too high for these radio jets to be produced by shocks in winds (See Section 4.2).

3. There are signs of jet interaction with the NLR (discussed further in Section 3). There is evidence that the kinematics and ionization of gas in the NLR is strongly influenced by

the linear radio sources [87,94,97–101]. This requires the radio source to be expanding into the ambient medium. In particular, the radio source in NGC 1068 (shown in Figure 1) and the central disk/torus are associated with outflows of ionized and molecular gas (e.g., [102–107]) and an X-ray emitting wind [108–111].

We note that the three arguments given here each apply to a relatively small number of sources; however, they paint a consistent picture that the linear radio sources are indeed jets.

2.3. Kpc-Scale Radio Structures (KSRs)

In addition to the radio jets seen on ∼10–100 pc scales, there is sometimes kpc-scale diffuse emission which is oriented out of the plane of the disk of the galaxy [112–118]. The radio emission is co-spatial with outflowing warm and hot gas [119,120]. The outflows are more consistent with being AGN-driven rather than starburst-driven based on energetics, polarization, and correlation of the radio and [OIII] λ5007 luminosity [115–118,121]. The outflows could be powered by radio jets that dissipate their energy in the ISM on sub-kpc scales [116] or by radiation from the AGN disk [41,118]. There is some evidence that the kpc-scale outflows are associated with the suppression of star formation in the host galaxy [118].

3. Evidence for Jet-Driven Outflows

Theoretical studies such as Gaspari et al. [122], Bourne and Sijacki [123], have predicted that mechanical feedback from AGN through jets can cause turbulence within 5–15 kpc of the center with a velocity dispersion in the outflowing gas of ∼200–400 km s^{-1}. In recent years, numerous studies utilizing 1D–3D spectroscopic observations have reported possible jet connections to these warm, ionized outflows.

3.1. Jet Interaction in the Emission Line Gas

Compact radio jets could strongly perturb the emission line gas along their axes [40,124]. Low z ($z < 0.6$) sources allow leveraging the high spatial resolution of radio interferometers and IFU to dissect the central a few kpc regions in 100 s of pc scales, where the compact jets strongly interact with their ambient medium. This is where studies at low z are useful for understanding the connection between the jets and outflows.

3.2. Kinematic Disturbance to the Emission Line Gas

Mullaney et al. [125] utilized 1D SDSS spectroscopic observations to investigate the primary process that shapes the kpc scale [O III]λ5007 emitting ionized gas kinematics. They fitted the optical emission lines in the wavelength range 4000–9000 Å with a multi-Gaussian model. They found that >30% of the AGN in their sample showed asymmetric line features in the [O III] emission line spectra and the line widths of the corresponding ionized gas clouds ($FWHM_{\rm avg}$) peak between the radio luminosity range, $L_{1.4\rm GHz} = 10^{23}$–10^{25} W Hz^{-1}. Mullaney et al. [125] stated that compact radio cores could induce turbulence in warm ionized gas, which manifests itself in large values of $FWHM_{\rm avg} > 1000$ km s^{-1}. However, they were unable to comment on the physical origin of the compact core due to the lack of spatial information. Other studies such as Heckman et al. [126], Whittle [127], Blundell and Beasley [128] have also concluded that compact radio sources could launch these ionized outflows, as the kinematically perturbed region in the ionized and molecular gas phases overlap with the radio emission, which often resembles a jet-like morphology [50]. Spectral studies of AGN have also proposed compact jet-driven outflows in AGN [129–131]. The study by Mullaney et al. [125] involved both RL and RQ AGN. Therefore, the narrow line region (NLR) gas clouds could experience kinematic disturbances in the RQ sources, not just in the RL AGN.

3.3. H I Absorption

In RL AGN the outflows are detected through asymmetric H I absorption profiles with velocities reaching up to ∼1500 km s^{-1} [132,133]. Strikingly, such high-velocity outflows

are rare in RQ AGN and have been detected in only a small number of sources. However, a number of low radio luminosity AGN are now known to also exhibit high-velocity H I outflows [134,135], indicating that H I outflows may originate in various conditions. These low luminosity sources represent a variety of circumstances, some of which obviously include radio jets [134,136], while others are likely the result of additional processes.

One such source is Mrk 231 where recent VLA observations by Morganti et al. [137] have confirmed the presence of a broad, blueshifted outflowing component in the H I absorption profile of Mrk 231, with $v_{\rm out} \sim 1300$ km s^{-1} and FWHM < 900 km s^{-1} [137]. The maximum spatial extension of this outflow is <1 kpc. Morganti et al. [137] suspected that either (1) the outflowing gas could be part of a flow distributed over a large opening angle, and located in front of the circumnuclear disk; or (2) the outflow relates to gas pushed out by the interaction with the radio bubble, in which case the absorption might occur against the southern radio bubble (or against the bubble and the core). The detection of H I in absorption requires a bright radio continuum source behind the atomic hydrogen. Since the RQ AGN has faint radio sources, it will be hard to detect H I in absorption. Therefore, there is a selection effect against the detection of H I in absorption in RQ AGN.

3.4. IFU Observations of Jet-Driven Outflows

Our understanding of the driving mechanism of the outflows and their coupling with the ISM in unresolved sources are benefited by spatially resolved studies of nearby galaxies which allow a detailed view of how jet/wind drive outflow or interact with the ISM. Numerous recent studies have included radio jets in RQ AGN and the kinematics of the multi-phase gas (observed in the ionized and molecular gas phases), where the common conclusion was that compact radio jets cause large disturbances in the ISM of host galaxies [39,49,50].

3.4.1. The Case of HE 1353-1917

Husemann et al. [49] recently observed a multi-phase kpc scale outflow in the edge-on galaxy HE 1353-1917. Despite the galaxy hosting an RQ AGN, we detected the radio emission to be co-spatial with the surface brightness profile for the H_2 [1-0 S(1)] λ21218Å, Brγ, Paβ and [Fe II] λ12570Å emission lines in Gemini-NIFS NIR observations. The velocity gradient along with the non-rotation of the ionized gas along the axis of the radio emission made the authors postulate that a radio jet could be connected to the outflow. The 10 GHz radio luminosity of the source is $L_{10\ \rm GHz} = 2 \times 10^{21}$ W Hz^{-1}. Assuming a range of possible radio spectral index (α), $-1.2 < \alpha < -0.5$, the corresponding 1.4 GHz radio luminosity (see Figure 2), $L_{1.4\rm GHz} = 5.3 \times 10^{21} - 2.5 \times 10^{22}$ W Hz^{-1}. The radio power vs. jet power scaling relation suggested by Cavagnolo et al. [138], estimates a jet power, $P_{\rm jet} = 3.3 \times 10^{43}$ erg s^{-1}. Spatially resolved observations of HE 1353-1917 suggested that the morphology of the multi-phase gas closely resembles an expanding shell-like shock front, rather than a homogeneously filled cone. Therefore, a thin-shell model could be much more appropriate to describe the geometry of the outflowing gas. The authors reported that the geometric shape of the shell with uniform thickness, $\Delta R = 5 - 500$ pc, returns a momentum injection rate, $\dot{p}_{\rm out} = 10^{33} - 2 \times 10^{34}$ dyne, and a kinetic energy injection rate, $\dot{E}_{\rm out} = 3 \times 10^{40} - 6 \times 10^{41}$ erg s^{-1}. The authors found that the injection of AGN momentum could only produce $\dot{p}_{\rm out}$ for high shell thickness, $\Delta R > 300$ pc. On the other hand, 10% of the jet power is sufficient to produce the observed $\dot{p}_{\rm out}$ and $\dot{E}_{\rm out}$. The spatial coincidence together with the outflow energetics suggests that the mechanical energy released from the radio jet could drive the outflows. However, 1% of the AGN bolometric luminosity ($L_{\rm bol} > 10^{44}$ erg s^{-1}) can describe $\dot{E}_{\rm out}$. Husemann et al. [49] suggested that the ambient gas shocked by the jet could face a secondary acceleration from the AGN-radiation field following a two-stage acceleration mechanism [139].

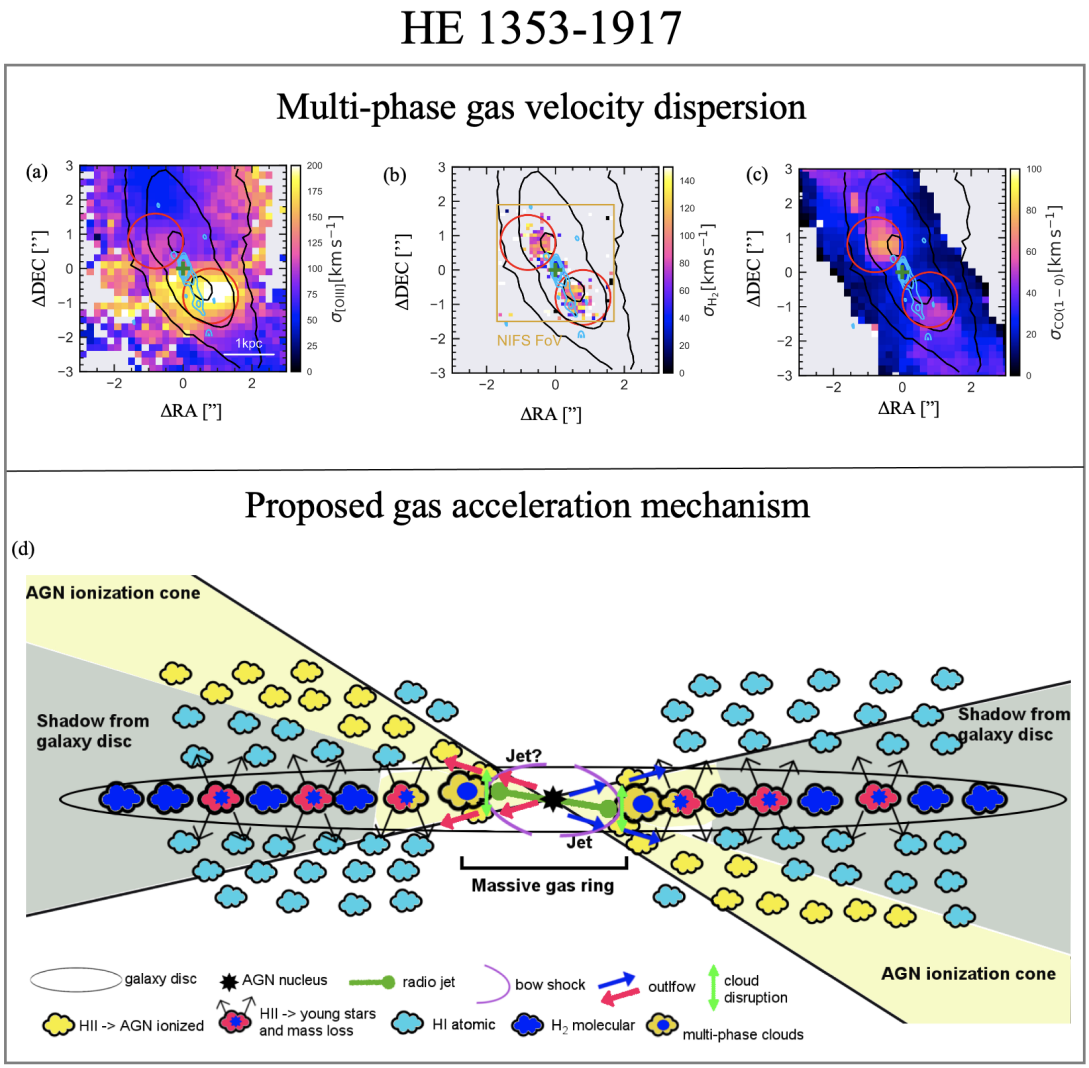

Figure 2. AGN-driven outflows in the RQ AGN HE 1353-1917, taken from Husemann et al. [49]. The 2D velocity dispersion maps of the multi-phase (**a**) ionized, (**b**) warm molecular, and (**c**) cold molecular gas overlaid with the VLA 10 GHz radio contour (in cyan). (**d**) Illustration of the proposed gas acceleration mechanism, in which the mechanical energy of the radio jet shock accelerates the ambient gas, which experiences a secondary re-acceleration by AGN radiation. However, only part of the gas receives the AGN radiation, as the rest is shadowed by the disk of the host galaxy. These findings suggest that more than one physical mechanism contributes to the multiple accelerations experienced by the outflowing gas.

3.4.2. Other Studies

In the Circinus galaxy, Elmouttie et al. [140] found that the radio jets are likely perturbing the gas above the core of Circinus and driving outflows with velocities <200 km s^{-1}. A study by Cecil et al. [141] reported five different streams with high-velocity dispersions ($\sigma_{out} \sim 200$ km s^{-1}) of the ionized gas filaments emerge from the CO ring in NGC 3079. The brightest stream is extended ∼250 pc along the axis of the VLBI radio jet to one corner of the superbubble's base and emits 10% of the Hα flux from the superbubble. GMRT observations by Hota and Saikia [142] detected H I gas co-spatial with the VLA radio continuum emission and H I absorption against the central radio peak at the systemic velocity of the galaxy in NGC 6764. The H I-absorption spectrum is suggestive of a possible weak absorption feature blueshifted by ∼120 km s^{-1}, indicating gas outflow. Chandra and XMM-Newton observations of Mrk 6 found hot X-ray emitting shocked gas around radio bubbles [143]. The temperature of the internal medium close to the bubbles was estimated

to be ∼0.9 keV, whereas the outer medium remains at ∼0.2 keV. This is consistent with a scenario where the gas in the shells is strongly shocking the interstellar medium (ISM) in the area. Alatalo et al. [144] reported molecular gas being driven out of NGC 1266 by a radio jet with velocities ∼ 180 km s^{-1}, causing net mass outflow rate of ∼2 $M_\odot$ yr^{-1} in the host galaxy. GMOS IFU observations Finlez et al. [145] detected ionized gas emission with two outflowing components ($\sigma_{\rm out} > 115$ km s^{-1}). The first component resides near the north-eastern and south-western radio lobes and is redshifted ($v_{\rm out} \sim 150$ km s^{-1}), and the second component is highly blueshifted ($v_{\rm out} \sim 250$ km s^{-1}) and is perpendicular to the axis of the radio jets. The authors suggested the redshifted component to be the jet-driven outflow, whereas the blueshifted component is an outflow originating from the accretion disk.

Jarvis et al. [39] found that the highly perturbed ionized gas spatially coincides with the radio jets in 10 $z < 0.2$ AGN with $L_{1.4\rm GHz} \sim 2 \times 10^{23} - 2.5 \times 10^{24}$ W Hz^{-1}. They estimated the velocity width of the [O III] that contains 80% of the total [O III] emission line flux (W_{80}) and observed an extremely high-value W_{80} (∼900–1200 km s^{-1}) in the vicinity of the radio jets, although most of the highest W_{80} regions in their observations are perpendicular to the jet axes. Girdhar et al. [50] focused on an RQ AGN at $z \sim 0.15$ and $L_{1.4\rm GHz} \sim 6 \times 10^{23}$ W Hz^{-1}. To estimate the emission line kinematics due to the jet-ISM interaction, the authors subtracted the stellar velocity dispersion (σ_*) contribution from the total emission line gas line width (W_{80}). They reported that the $W_{80} - 2.6\,\sigma_*$ value is the highest (<1300 km s^{-1}) on the perpendicular to the axis of the radio jet. On the axis of the jet $W_{80} - 2.6\,\sigma_*$ decreases to ∼400 km s^{-1}. The region of the highest $W_{80} - 2.6\,\sigma_*$ also coincides with the AGN ionization cone. Studies by Venturi et al. [40], Morganti et al. [136] on Seyfert 2 galaxies such as NGC 1068 and IC 5063 have also found that AGN with lower radio luminosity ($L_{5\rm GHz} \sim 7 \times 10^{22}$–$9 \times 10^{23}$ W Hz^{-1}) could harbor radio jets, which could drive multi-phase gas outflows. The jet origin of the radio emission was based on the core and lobe morphology seen in VLA 5 GHz radio observations.

4. AGN Winds

4.1. Thermal Free–Free Emission

Blundell and Kuncic [45] proposed a model where the thermal energy of the accretion disk drives the outflows and the free–free emission mainly contributes to the observed radio emission on sub-pc scale. The authors stated that the flat spectrum of compact radio cores in RQ AGN is due to the AGN wind. The wind is launched at a radius ($r_{\rm w}$), called the launch radius of the AGN wind. Within this radius, the outflows could be dominated by the Poynting flux and form jets. The electron density ($N_{\rm e}$) could be related to the mass outflow rate by the AGN wind ($\dot{M}_{\rm w}$):

$$N_{\rm e} = 1 \times 10^{12} \bar{g}_{10} f_{\Omega,\,0.1}^{-1} \left(\frac{\dot{M}_{\rm w}}{M_\odot {\rm yr}^{-1}}\right) \left(\frac{v_{\rm w}}{500\ {\rm km\ s^{-1}}}\right)^{-1} \left(\frac{r_{\rm w}}{10^{15}\ {\rm cm}}\right)^{-1} {\rm cm}^{-3} \quad (1)$$

where $\bar{g}_{10} = g_{\rm ff}/10$, and $g_{\rm ff}$ being the gaunt factor, $f_{\Omega,\,0.1} = f_\Omega/10$, f_Ω is the geometric covering factor that could be written as $\Omega/4\pi$ (Ω is the solid angle), $v_{\rm w}$ is the speed of the AGN wind. We assume $g_{\rm ff} = 1$, $v_{\rm w} = 1000$ km s^{-1} as per King [146], Zubovas and King [147].

$$L_{\nu,\Omega} = 3 \times 10^{20} \bar{g}_{10} T_7^{-1/2} f_{\Omega,\,0.1}^{-2} \left(\frac{\dot{M}_{\rm w}}{M_\odot {\rm yr}^{-1}}\right)^2 \left(\frac{v_{\rm w}}{500\ {\rm km\ s^{-1}}}\right)^{-2} \left(\frac{r_{\rm ph}}{0.1\ {\rm pc}}\right)^{-1} {\rm W\ Hz\ sr}^{-1} \quad (2)$$

where $T_7 = T_e/10^7$K and r_{ph} is the photospheric radius, the radius at which the outflow becomes transparent [148]. Blundell and Kuncic [45] suggested that the value of r_{ph} ranges between 0.1–1 pc in general.

4.2. Synchrotron Emission from the Winds

Zakamska and Greene [41] proposed that the AGN-driven wind can shock accelerate the relativistic electrons in the plasma and cause radio emission—see the discussion of diffuse kpc-scale radio emission in Section 2.3. In their model, the AGN wind flows in all directions, but it takes the path of least resistance and escapes. In their model, the radio emission will be diffuse and extended on kpc-scales. The authors argued that the 12 µm infrared radiation originates from the dust heating by the photons from the AGN accretion disk. The correlation between the 12 µm luminosity, radio luminosity, and the line width of the emission line gas is suggestive of the outflows to be driven by AGN winds. In their model, the wind shock accelerates the ambient medium and results in synchrotron emission on kpc scales. Low-resolution radio interferometric observations may detect extended radio emissions on kpc scales. However, zooming into that radio emission on sub-kpc scales with higher resolution will provide non-detection of compact knots, if the radio emission is truly diffuse. Liu et al. [149] used VLBA observations to zoom in the central $1'' \times 1''$ region of a z = 5 AGN J2242+0334. which could not be resolved by previous VLA observations. Previous 1.5 and 3 GHz VLA observations by Liu et al. [150], estimated a minimum resolvable size ∼2.3 kpc; however, the VLBA observation did not show any detection of radio emission. One interpretation of this finding is the existence of an AGN-driven wind that is extended on kpc scales. Star formation processes cannot describe this radio emission, as the radio-derived SFR is >20 times higher than the maximum IR-derived SFR. Liu et al. [149] left the possibility of radio emission being produced by the interaction between a weak jet and its ambient medium. Accretion disk winds are thought to play a key role in launching the outflows in low luminosity ($L_{5GHz} < 10^{22.8}$ W Hz^{-1}), RQ AGN [46].

4.3. Relation to the Outflows

Woo et al. [38] investigated a large sample (∼39,000), local ($z < 0.3$), and obscured AGN. They found that ∼45% of type 2 AGN at $z < 0.3$ exhibit asymmetry in the [O III] emission lines, thereby suggesting observational evidence of warm, ionized gas outflows. The authors reported that the ionized gas velocity dispersion increases with the AGN bolometric luminosity and Eddington ratio. Woo et al. [151], Rakshit and Woo [152] have also reported a similar trend in a sample of >110,000 $z < 0.3$ AGN, where the authors concluded that radiation pressure or winds could power the outflows. However, the winds could be either the radiatively driven [153,154], thermally driven [155] or magnetically driven [156], implying that winds cannot be synonymous with radiation pressure. These winds could also be either energy or momentum-conserving. A theoretical study by Faucher-Giguère and Quataert [157] suggested that AGN would power ultra-fast outflows (UFOs) with velocities, $v_{out} \sim 0.1c$. Recent studies of PG 1211+143 and PDS 456 have found that magnetohydrodynamic (MHD) winds are the key driver of UFOs. The slower winds of $v_{out} < 1000$ km s^{-1} are likely to be driven by the radiation pressure on dust [157]. This great diversity in accretion disk-driven winds can only be explored by combining multi-wavelength high-resolution IFU and imaging observations, which may put observational constraints on theoretical predictions.

4.4. Observational Evidence of Wind-Driven Outflows in Mrk 1044

The nearby (z = 0.016), narrow-line Seyfert galaxy Mrk 1044 hosts a luminous ($L_{bol} = 1.4 \times 10^{44}$ erg s^{-1}), super-Eddington (Eddington ratio, $\lambda_{Edd} > 2$), and RQ AGN [158]. A recent study using MUSE WFM observation [159] found that the ionized gas outflow in [O III] is unresolved, with the outflow contained within the central 600 pc radius. The velocity of the outflowing gas, $v_{out} = -452 \pm 5$ km s^{-1}, and the velocity dispersion, $\sigma_{out} = 287 \pm 5$ km s^{-1} indicate a kinematic disturbance in the ambient medium due to

AGN-driven outflows. Winkel et al. [160] used the UV Space Telescope Imaging Spectrograph (STIS) at the Hubble Space Telescope (HST) and the optical MUSE Narrow Field Mode (NFM) observations to understand the ionized gas outflow properties at UV and optical wavelengths in greater detail. The Ly α absorption lines in the UV reveal two outflowing components L1 and L2, with $v_{\rm out}$ being $v_{\rm out,L1} = -278 \pm 36$ km s^{-1} and $v_{\rm out,L2} = -1118 \pm 2$ km s^{-1} respectively. On the other hand, the optical data show three outflowing components H0, O1, and O2, which are all visible in Hβ, [O III], and Hα. Whereas the Balmer emission lines are more prominent in the H0 component, the forbidden [O III] is the brightest in the O1 and O2 components. The H0 outflow is spatially resolved with an extension $R_{\rm out,H0} = 4.6 \pm 0.6$ pc, with moderate outflow velocities ($v_{\rm out,H0} = -211 \pm 22$ km s^{-1}). O1 and O2 on the other hand are spatially unresolved $R_{\rm out,O1-O2} < 1.7$ pc. Similarly to H0, O1 is slightly blueshifted ($v_{\rm out,O1} = -211 \pm 22$ km s^{-1}); while O2 shows a significant blue shift ($v_{\rm out,O2} = -560 \pm 20$ km s^{-1}). The VLA 6 and 10 GHz radio observations show compact radio structures extended on <50 pc scales (see Figure 3), with a spectral index of $\alpha = -0.61 \pm 0.16$. Winkel et al. [160] mentioned that star formation processes could in principle power the ionized outflow; however, the observed outflow could also be driven by the AGN, as 0.2% of $L_{\rm bol}$ is sufficient to reproduce the observed $\dot{E}_{\rm out} = 7.3 \times 10^{41}$ erg s^{-1}.

This is where multi-wavelength studies of AGN-driven outflows are so important. X-ray wavelengths could provide us with information that is not available from optical and UV. Ultra-fast outflows (UFOs) with $v_{\rm out}$ > 10,000 km s^{-1} in X-rays trace the highest ionization gas experiencing AGN activity on the accretion disk scales. Krongold et al. [161] used XMM-Newton EPIC-pn camera and the RGS instrument. EPIC-pn observation reveals highly ionized absorption lines, such as Fe XXII, Ni XXII+, etc., and three different UFO components (UFO1-3). Spectroscopic analysis of the RGS spectra demonstrates that different UFO components are in different ionization states. For example, the ionization parameter U [162] in UFO1 is substantially higher ($\log U_{\rm UFO1} = 2.4 \pm 0.1$) than UFO3 ($\log U_{\rm UFO3} = -2.9 \pm 0.1$). The velocity of the X-ray emitting gas clouds in UFO1 ($v_{\rm out,UFO1}$ = 44,790 km s^{-1}) is about twice those of UFO3 ($v_{\rm out,UFO3}$ = 23,610 km s^{-1}). However, the hydrogen column densities of ($N_{\rm H}$) these two outflowing components differ by three orders of magnitude ($N_{\rm H,UFO1} \sim 10^{23}$ cm^{-2} and $N_{\rm H,UFO3} \sim 10^{20}$ cm^{-2}). Krongold et al. [161] stated that such discrepancies in ionization states, kinematics, and column densities strongly suggest a multi-phase structure of the gas. Longinotti et al. [163] showed that plums of gas with velocities similar to UFOs are formed due to instabilities in the UFOs. The highly ionized component (UFO1) is the shocked outflow due to accretion disk winds, whereas the outflowing gas in lower ionization states (UFO3) forms due to the instabilities in the UFO during the entrainment of cold materials. If a similar mechanism drives the multi-phase gas outflows from hot X-ray emission to cold molecular gas phases, then the accretion disk wind in Mrk 1044 drives the ionized gas outflows at optical and UV wavelengths.

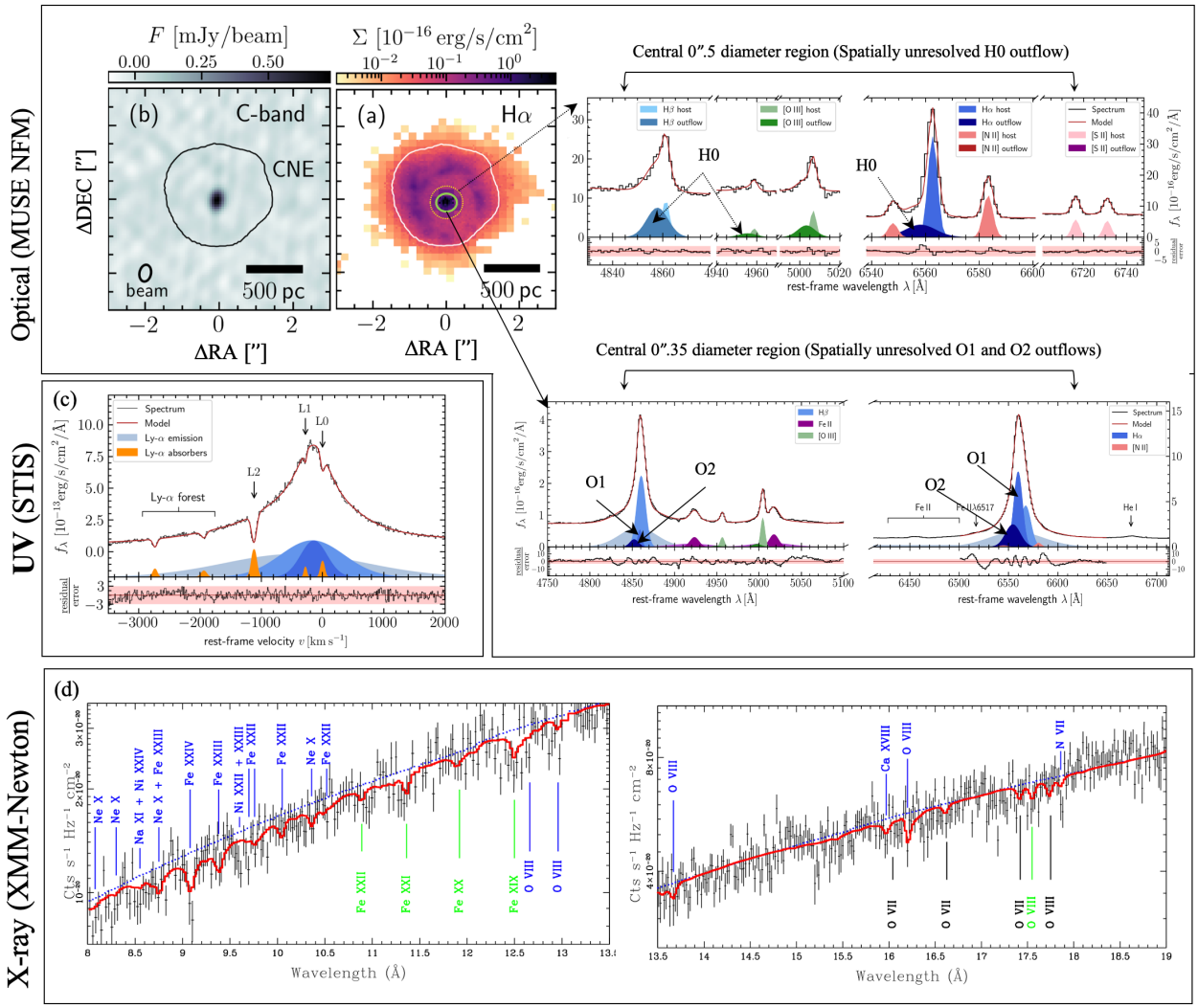

Figure 3. Multi-phase outflow in Mrk 1044, where the optical and UV results are taken from Winkel et al. [160] and the X-ray counterpart is taken from Krongold et al. [161] (© AAS. Reproduced with permission). Optical: (**a**) Hα surface brightness map overlaid with the MUSE WFM PSF (white contour). The 0″.35 and 0″.5 diameter regions are indicated by the yellow and green circles, respectively. In the right panels, we can observe the Hβ+[OIII] and Hα+[NII] spectra extracted from the central 0″.35 (top right panel) and 0″.5 (bottom right panel) diameter regions, as denoted by the circles. The H0 outflow is spatially resolved and has a spatial extension of 4.6 pc. O1 and O2 outflows on the other hand are spatially unresolved with predicted spatial extensions <1.7 pc. (**b**) VLA 6 GHz radio continuum image overlaid with the MUSE PSF (black contour). (**c**) Modelling the UV-spectrum of Mrk 1044 (top panel), along with the normalized residuals (bottom panel). The fact that the residuals fall within the 3σ uncertainty range indicates that the spectral model (in red) accurately represents the observed spectrum (in black). Aside from the Ly α forest, two outflowing systems L1 and L2 are seen. L0 corresponds to the rest frame of the host galaxy. The boundary of the MUSE PSF corresponds to the circumnuclear ellipse (CNE). XMM-Newton RGS spectra within (**c**) 8–13.5 Å, and (**d**) 13.5–19 Å showing high ionization absorption lines which is a signature of the UFO.

4.5. Other Studies

A study by Liu et al. [164] studied 11 $z \sim 0.5$ and luminous ($L_{\rm bol} > 10^{46}$ erg s^{-1}) RQ quasars using GMOS IFU reported ionized outflows with a median outflow velocity of 760 km s^{-1}, which are either very similar to or above the escape velocities from the host galaxies. The authors suggested that these outflows are likely driven by quasar winds and they correspond to mass outflow rates $\dot{M}_{\rm out}$ = 2000–20,000 $M_\odot$ and kinetic energy

injection rates $\dot{E}_{\rm kin} = 4 \times 10^{44} - 3 \times 10^{45}$ erg s^{-1}. Such large values of $\dot{M}_{\rm out}$ and $\dot{E}_{\rm kin}$ could significantly affect their host galaxies' evolution. A study of 7 $L_{\rm bol} > 10^{44}$ erg s^{-1}, z $\sim$ 0.1 type II AGN by McElroy et al. [29] found spatially resolved outflows, where the mean $W_{80} = 790 \pm 90$ km s^{-1}, with W_{80} values reaching a maximum of 1600 km s^{-1}. MUSE observations of background quasars by [165] found 6 Mg II host galaxies at z = 0.8–1.4 where outflow velocities only reach up to 150 km s^{-1}, which is smaller than the escape velocities from their host galaxies. In this case, the outflows may not be powerful enough to quench star formation over kpc scales.

5. A Systematic Statistical IFU Study

Singha et al. [159] analyzed the IFU observations (VLT/MUSE and VIMOS) of 36 nearby ($0.01 < z < 0.06$), luminous (10^{43}erg s^{-1} $< L_{\rm bol} <$ 10^{46}erg s^{-1}), and RQ AGN from the Close AGN Reference Survey (CARS) AGN sample [166,167]. The authors performed a spectro-astrometric analysis and found that most ($\sim$63%) of the AGN in their sample exhibit compact/unresolved outflows (see Figure 4), where the maximum [O III] wing emitting region is located at <100 pc ($S_{[\rm O\ III]}$) from the nucleus. These offsets could imply that the outflow has been extended to a distance of ($S_{[\rm O\ III]} < 100$ pc) from the nucleus or the warm, ionized gas phase of the multi-phase outflow starts emitting in [O III] at ($S_{[\rm O\ III]} < 100$ pc). Additionally, Singha et al. [159] reported that the AGN with compact outflows has a very similar $L_{\rm bol}$ compared to the AGN with extended outflows (possibly extended on several kpc scales). This means that other parameters, such as the AGN duty cycle time scale or radio properties, could dictate whether the outflows will be confined to the central 1 kpc region or extended over several kpc scales.

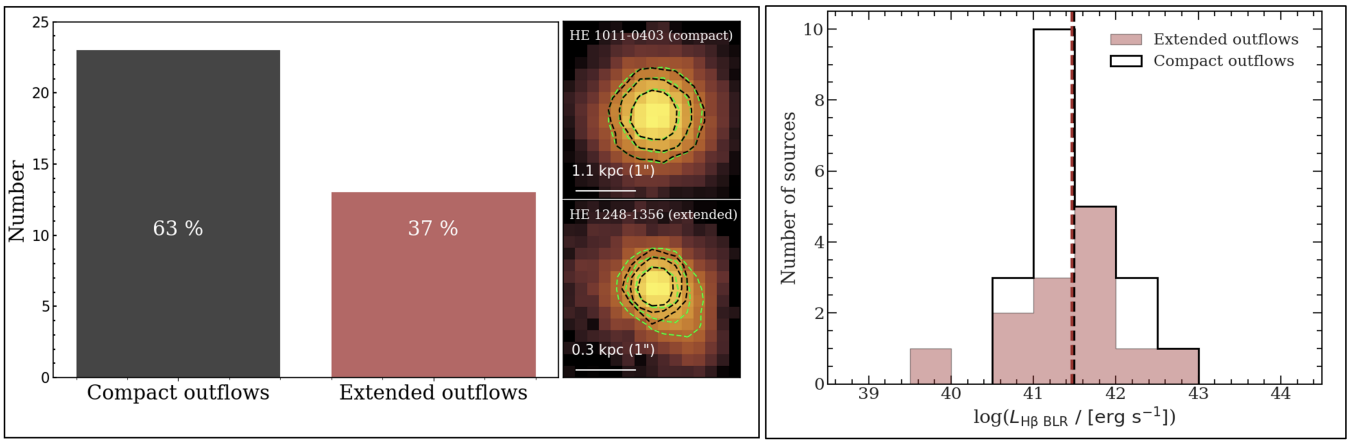

(**a**) (**b**)

Figure 4. Results from the work of Singha et al. [159]. (**a**) A bar chart showing the percentages of compact/unresolved and extended/resolved outflows, along with the 2D flux distributions of representative AGN. (**b**) Histograms of the BLR H β luminosities for AGN with compact and extended outflows. The vertical lines denote their mean broad line region (BLR) Hβ luminosities, which appear similar. These results suggest that the AGN accretion properties may not solely drive the outflows.

6. Recent JWST Observations: The Case of XID 2028

Spatially resolved observations at infrared (IR) wavelengths provide an invaluable opportunity to dissect regions dominated by star formation, shocks, and AGN photoionization. With the introduction of JWST, the superior sensitivity together with the high angular resolution, we can now explore the plethora of information studying the emission features in the 1–27 µm wavelength regime. It also enables us to investigate the feedback process of AGN at cosmic noon. The Near-Infrared Spectrograph [168] on the James Webb Space Telescope (JWST/NIRSpec) has recently observed an RQ AGN XID 2028 (PI: D. Wylezalek). The 3″ $\times$ 3″ FoV of NIRSpec combined with a PSF FWHM of 0.045″ provides an angular

resolution of ∼300 pc to study the AGN feedback from sub-kpc to several kpc scales at its redshift, z = 1.59. The near-infrared wavelength covers the [O III]λ5007 crucial around 1.3 µm at this redshift.

A 3D spectroscopic analysis by Cresci et al. [169] revealed numerous kinematically distinct regions—(i) highly blueshifted outflowing gas with velocity (v), -1000 km s^{-1} $< v$, (ii) filamentary structures that seemingly connect the AGN to the blueshifted outflow (-1000 km s^{-1} $< v < -600$ km s^{-1}), (iii) red-shifted outflow (-600 km s^{-1} $< v < -250$ km s^{-1}). The bluest part of the outflow (approaching side) reaches a velocity of -1000 km s^{-1}, where the redshifted outflowing gas (receding side) exhibits a similar velocity (∼+800 km s^{-1}). The similarity of velocities on the approaching and the receding sides and their locations on the opposite sides of the AGN suggest a biconical outflow geometry. Such geometrical structures of the outflowing ionized gas are not totally unprecedented. Over the last two decades numerous studies have reported bi-conical geometry in outflowing multi-phase gas in many sources such as NGC 2992 [170], Mrk 573 [171], NGC 252 [172], and NGC 5728 [173], etc.

The velocity gradient from the filaments towards the outflow, on the other hand, is suggestive of a physical connection between them. The ionized outflowing [O III]λ5007 gas shows a high line width, $\sigma_{\rm out} \sim 450$ km s^{-1}, indicating kinematic disturbance in the narrow line gas clouds.

Although categorized as an RQ AGN by Perna et al. [174], 3 GHz Very Large Array (VLA) observations [175] have revealed two radio blobs. Vardoulaki et al. [175] categorized XID 2028 as a star-forming galaxy. Cresci et al. [169] pointed out that the peak of radio emission is offset from the AGN, which is not consistent with a star-forming origin of radio emission. The spatial coincidence of the radio blobs with both the approaching and receding sides of the outflow hints towards the jet origin of the blobs and therefore a jet connection to the AGN-driven outflow. The filamentary structures could be a hot expanding bubble filled with low-surface-brightness emission that is edge-brightened. The MOKA^{3D} model by Cresci et al. [169] suggests that the geometry of the observed ionized gas could be easily reproduced by an expanding bubble, which is dragged by the jets and winds (see Figure 5), and a collimated outflow towards the direction of the jet propagation, where the jets could break out from its host galaxy. Their model is consistent with the simulations of Gaibler et al. [176], where the expanding bubbles and jets could excavate cavities in the disk of the galaxy and trigger star formation at the edges of the shell. At a 6 kpc radius, the jets penetrate the bubble and traverse through the low-density ISM together with the AGN wind, eventually creating a collimated outflow. Veilleux et al. [177] performed an independent analysis of the ionized gas outflows and found similar results. However, they left the possibility open that the radio emission could entirely be non-thermal synchrotron emission due to the fast-moving plasma as a result of the shocked ionized gas by the AGN wind.

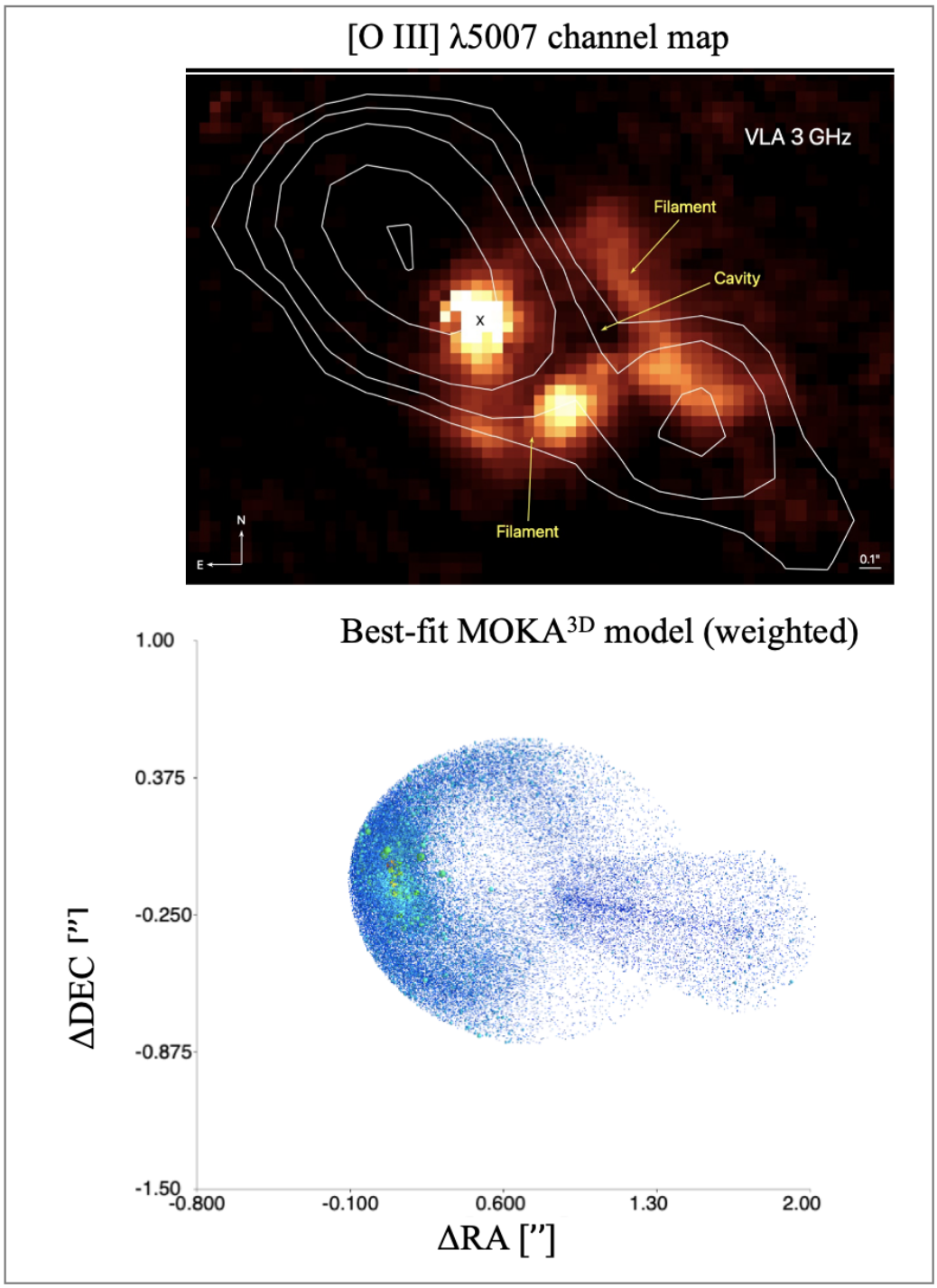

Figure 5. JWST/NIRSpec results from the work of Cresci et al. [169]. *Upper panel:* [O III]λ5007 map of the sector where the filamentary structures are the most prominent, overlaid with VLA 3 GHz radio contours (in white). *Lower panel:* MOKA^{3D} model showing the expanding bubble and the collimated jet. The clouds are weighted based on the fluxes and kinematics at their locations. These results show that outflows are accelerated by both winds and jets, rather than just one of them.

7. Summary and Conclusions

We review the potential driving mechanism of the ionized gas outflows in the RQ AGN, paying special attention to the processes connected to radio emission. From sub-pc to sub-kpc scales, the gas outflows propagate through a multi-phase medium. Among those, the warm, ionized gas outflows are the most energetic gas phase that could be spatially

resolved with the current high-resolution imaging and IFU capabilities. The fundamental nature of radio emissions and their connections to these outflows are currently strongly debated. Two leading hypotheses of driving outflows are (i) AGN winds and (ii) radio jets. The key takeaway points are as follows.

- Radio-interferometric observations have detected both jets and winds in RQ AGN. The evidence for jets consists of (1) structures which are self-similar with those of sources in RL AGN, (2) proper motions in some sources, and (3) disturbances in the ambient gas due to the propagating radio sources. Jets are collimated and exhibit linear structures with cores and sometimes lobes. The radio mission due to AGN winds are expected to be extended and diffuse in VLA images; in addition, because the emission is diffuse, no compact structure should be detected in VLBA images of winds (Section 2).
- Low-power radio jets have been believed to strongly perturb ambient gas and drive outflows, as seen in different spectroscopic studies. In the nearby RQ AGN HE 1353-1917, a collimated radio jet-like structure not only spatially coincides with the multi-phase gas outflows, but also it is powerful enough to drive the outflows. However, the acceleration mechanism of the outflow is likely a two-step process in which both the radio jet and the AGN-radiation field participate (Section 3).
- The winds from AGN could propagate on the kpc scales and generate shocks which give rise to non-thermal emission. In this case, the radio continuum emission is expected to be diffuse. An example of a multi-phase outflow could be found in a $z < 0.02$ AGN Mrk 1044. Multiple outflowing gas components with velocities ranging from 100–40,000 km s^{-1}, show a great diversity in their ionization states and column densities. The outflows are contained within the central 5 pc region. Theoretical models suggest that AGN-driven winds give rise to highly ionized outflowing gas. Outflowing ionized gas clouds which are at a lower ionization state, originate from various instabilities developed on the boundaries of the shocked outflow (Section 4).
- Ionized gas outflows in local ($0.01 < z < 0.06$) RQ AGN are mostly spatially unresolved, and the brightest part of the ionized gas outflows have projected offsets <100 pc from the AGN. Furthermore, the unresolved and resolved (extended outflows) have very similar $L_{\rm bol}$, suggesting that the luminous AGN may not launch large-scale outflows. Their radio properties and AGN duty cycles can affect the spatial extension of the outflows (Section 5).
- The high angular resolution and the sensitivity of JWST enable one to resolve the ionized gas outflows at cosmic noon spatially. Recent JWST/NIRSpec observation of RQ AGN XID 2028 has revealed a biconical outflow with velocities reaching about 1000 km s^{-1}, where the AGN connects to the approaching and receding sides through edge-brightened filaments. The spatial coincidence of radio jets with the outflow could be explained by an expanding bubble and the jets creating cavities and triggering star formation on the bubble edge. On the kpc scales, the jet penetrates the bubble and escapes the host galaxy.

In this review, we show that it is not just radio jets or winds that could drive the ionized gas outflows but that both jets and winds could play a role. It is now imperative to study the central 1 kpc region of the RQ AGN with high-resolution interferometric observation to understand the morphology of the observed radio emission, and the ionized gas kinematics across the electromagnetic spectrum utilizing the high-resolution imaging and IFU capabilities of HST and JWST. Furthermore, numerical simulations taking account of multiple outflow driving mechanisms are key to understanding the complex ionized gas kinematics from sub-pc to kpc scales, on which future observations could place constraints. Concluding whether a radio emission blob represents a relic of a past jet/lobe or diffuse emission from the AGN wind is not trivial. Only through investigations of the jet-ISM interaction across radio continuum, X-ray, optical IFU spectroscopy, and molecular gas kinematics can unveil the role and the effect of their interplay. Sources such as Minkowski's object, the death star galaxy, or RAD12 are essential to guide the numerical simulations.

Detailed studies at high redshifts, facilitated by the recent launch of JWST, are already unraveling intricacies that once reached solely for nearby galaxies two decades past.

Author Contributions: All authors contributed to the writing of the article. All authors have read and agreed to the published version of the manuscript.

Funding: This work was supported by the Natural Sciences and Engineering Research Council (NSERC) of Canada.

Data Availability Statement: Not applicable.

Conflicts of Interest: The authors declare no conflict of interest.

Abbreviations

The following abbreviations are used in this manuscript:

ΛCDM	Lambda Cold Dark Matter
AGN	Active Galactic Nuclei
BLR	Broad Line Region
CARS	Close AGN Reference Survey
CNE	Circumnuclear Ellipse
FWHM	Full Width to Half Maximum
GMOS	Gemini (South) Multi-Object Spectrograph
HST	Hubble Space Telescope
IFU	Integral Field Unit
IGM	Intergalactic Medium
ISM	Interstellar Medium
JWST	James Webb Space Telescope
Jy	Jansky
MERLIN	Multi-Element Radio-Linked Interferometer Network
MUSE	Multi-Unit Spectroscopic Explorer
NFM	Narrow Field Mode
NIRSpec	Near-Infrared Spectrograph
NLR	Narrow Line Region
PSF	Point Spread Function
RGS	Reflection Grating Spectrometer
RL	Radio Loud
RQ	Radio Quiet
SDSS	Sloan Digitized Sky Survey
SMBH	Super-Massive Black Hole
UFO	Ultra-Fast Outflow
UV	Ultra-violet
VIMOS	Visible Multi Object Spectrograph
VLA	Very Large Array
VLBA	Very Long Baseline Array
VLT	Very Large Telescope
WFM	Wide Field Mode

References

1. Cattaneo, A.; Faber, S.M.; Binney, J.; Dekel, A.; Kormendy, J.; Mushotzky, R.; Babul, A.; Best, P.N.; Brüggen, M.; Fabian, A.C.; et al. The role of black holes in galaxy formation and evolution. *Nature* **2009**, *460*, 213–219.
2. Alexander, D.M.; Hickox, R.C. What drives the growth of black holes? *New Astron. Rev.* **2012**, *56*, 93–121.
3. Fabian, A.C. Observational Evidence of Active Galactic Nuclei Feedback. *Annu. Rev. Astron. Astrophys.* **2012**, *50*, 455–489.
4. McNamara, B.R.; Nulsen, P.E.J. Mechanical feedback from active galactic nuclei in galaxies, groups and clusters. *New J. Phys.* **2012**, *14*, 055023.
5. Heckman, T.M.; Best, P.N. The Coevolution of Galaxies and Supermassive Black Holes: Insights from Surveys of the Contemporary Universe. *Annu. Rev. Astron. Astrophys.* **2014**, *52*, 589–660.
6. Heckman, T.M.; Best, P.N. A Global Inventory of Feedback. *Galaxies* **2023**, *11*, 21.
7. Couto, G.S.; Storchi-Bergmann, T. The Interplay between Radio AGN Activity and Their Host Galaxies. *Galaxies* **2023**, *11*, 47.

8. Silk, J.; Rees, M.J. Quasars and galaxy formation. *Astron. Astrophys.* **1998**, *331*, L1–L4.
9. Ferrarese, L.; Merritt, D. A Fundamental Relation between Supermassive Black Holes and Their Host Galaxies. *Astrophys. J.* **2000**, *539*, L9–L12.
10. Merritt, D.; Ferrarese, L. The M-σ Relation for Supermassive Black Holes. *Astrophys. J.* **2001**, *547*, 140–145.
11. Magorrian, J.; Tremaine, S.; Richstone, D.; Bender, R.; Bower, G.; Dressler, A.; Faber, S.M.; Gebhardt, K.; Green, R.; Grillmair, C.; et al. The Demography of Massive Dark Objects in Galaxy Centers. *Astron. J.* **1998**, *115*, 2285–2305.
12. Gültekin, K.; Richstone, D.O.; Gebhardt, K.; Lauer, T.R.; Tremaine, S.; Aller, M.C.; Bender, R.; Dressler, A.; Faber, S.M.; Filippenko, A.V.; et al. The M-σ and M-L Relations in Galactic Bulges, and Determinations of Their Intrinsic Scatter. *Astrophys. J.* **2009**, *698*, 198–221.
13. Benson, A.J.; Bower, R.G.; Frenk, C.S.; Lacey, C.G.; Baugh, C.M.; Cole, S. What Shapes the Luminosity Function of Galaxies? *Astrophys. J.* **2003**, *599*, 38–49.
14. Croton, D.J.; Springel, V.; White, S.D.M.; De Lucia, G.; Frenk, C.S.; Gao, L.; Jenkins, A.; Kauffmann, G.; Navarro, J.F.; Yoshida, N. The many lives of active galactic nuclei: Cooling flows, black holes and the luminosities and colours of galaxies. *Mon. Not. R. Astron. Soc.* **2006**, *365*, 11–28.
15. Bower, R.G.; Benson, A.J.; Crain, R.A. What shapes the galaxy mass function? Exploring the roles of supernova-driven winds and active galactic nuclei. *Mon. Not. R. Astron. Soc.* **2012**, *422*, 2816–2840. [CrossRef]
16. Baum, S.A.; O'Dea, C.P. Multifrequency VLA observations of PKS 0745-191: The archetypal "cooling flow" radio source? *Mon. Not. R. Astron. Soc.* **1991**, *250*, 737. [CrossRef]
17. McNamara, B.R.; Nulsen, P.E.J. Heating Hot Atmospheres with Active Galactic Nuclei. *Annu. Rev. Astron. Astrophys.* **2007**, *45*, 117–175.
18. Gaspari, M.; Sądowski, A. Unifying the Micro and Macro Properties of AGN Feeding and Feedback. *Astrophys. J.* **2017**, *837*, 149.
19. Cicone, C.; Brusa, M.; Ramos Almeida, C.; Cresci, G.; Husemann, B.; Mainieri, V. The largely unconstrained multiphase nature of outflows in AGN host galaxies. *Nat. Astron.* **2018**, *2*, 176–178.
20. Singha, M.; O'Dea, C.P.; Gordon, Y.A.; Lawlor-Forsyth, C.; Baum, S.A. Ionized Gas Outflows in Low-excitation Radio Galaxies Are Radiation Driven. *Astrophys. J.* **2021**, *918*, 65.
21. Forman, W.; Jones, C.; Churazov, E.; Markevitch, M.; Nulsen, P.; Vikhlinin, A.; Begelman, M.; Böhringer, H.; Eilek, J.; Heinz, S.; et al. Filaments, Bubbles, and Weak Shocks in the Gaseous Atmosphere of M87. *Astrophys. J.* **2007**, *665*, 1057–1066.
22. Tombesi, F.; Cappi, M.; Reeves, J.N.; Palumbo, G.G.C.; Yaqoob, T.; Braito, V.; Dadina, M. Evidence for ultra-fast outflows in radio-quiet AGNs. I. Detection and statistical incidence of Fe K-shell absorption lines. *Astron. Astrophys.* **2010**, *521*, A57.
23. Tombesi, F.; Cappi, M.; Reeves, J.N.; Palumbo, G.G.C.; Braito, V.; Dadina, M. Evidence for Ultra-fast Outflows in Radio-quiet Active Galactic Nuclei. II. Detailed Photoionization Modeling of Fe K-shell Absorption Lines. *Astrophys. J.* **2011**, *742*, 44.
24. Tombesi, F.; Cappi, M.; Reeves, J.N.; Nemmen, R.S.; Braito, V.; Gaspari, M.; Reynolds, C.S. Unification of X-ray winds in Seyfert galaxies: From ultra-fast outflows to warm absorbers. *Mon. Not. R. Astron. Soc.* **2013**, *430*, 1102–1117.
25. Arav, N.; Korista, K.T.; Barlow, T.A.; Begelman. Radiative acceleration of gas in quasars. *Nature* **1995**, *376*, 576–578. [CrossRef]
26. Arav, N.; Borguet, B.; Chamberlain, C.; Edmonds, D.; Danforth, C. Quasar outflows and AGN feedback in the extreme UV: HST/COS observations of HE 0238-1904. *Mon. Not. R. Astron. Soc.* **2013**, *436*, 3286–3305.
27. Arav, N.; Xu, X.; Miller, T.; Kriss, G.A.; Plesha, R. HST/COS Observations of Quasar Outflows in the 500–1050 Å Rest Frame. I. The Most Energetic Outflows in the Universe and Other Discoveries. *Astrophys. J. Suppl. Ser.* **2020**, *247*, 37.
28. Harrison, C.M.; Alexander, D.M.; Mullaney, J.R.; Swinbank, A.M. Kiloparsec-scale outflows are prevalent among luminous AGN: Outflows and feedback in the context of the overall AGN population. *Mon. Not. R. Astron. Soc.* **2014**, *441*, 3306–3347.
29. McElroy, R.; Croom, S.M.; Pracy, M.; Sharp, R.; Ho, I.T.; Medling, A.M. IFU observations of luminous type II AGN—I. Evidence for ubiquitous winds. *Mon. Not. R. Astron. Soc.* **2015**, *446*, 2186–2204.
30. Kang, D.; Woo, J.H. Unraveling the Complex Structure of AGN-driven Outflows. III. The Outflow Size-Luminosity Relation. *Astrophys. J.* **2018**, *864*, 124.
31. Aalto, S.; Garcia-Burillo, S.; Muller, S.; Winters, J.M.; van der Werf, P.; Henkel, C.; Costagliola, F.; Neri, R. Detection of HCN, HCO^+, and HNC in the Mrk 231 molecular outflow. Dense molecular gas in the AGN wind. *Astron. Astrophys.* **2012**, *537*, A44.
32. Combes, F.; García-Burillo, S.; Casasola, V.; Hunt, L.; Krips, M.; Baker, A.J.; Boone, F.; Eckart, A.; Marquez, I.; Neri, R.; et al. ALMA observations of feeding and feedback in nearby Seyfert galaxies: An AGN-driven outflow in NGC 1433. *Astron. Astrophys.* **2013**, *558*, A124.
33. Cicone, C.; Maiolino, R.; Sturm, E.; Graciá-Carpio, J.; Feruglio, C.; Neri, R.; Aalto, S.; Davies, R.; Fiore, F.; Fischer, J.; et al. Massive molecular outflows and evidence for AGN feedback from CO observations. *Astron. Astrophys.* **2014**, *562*, A21.
34. Dall'Agnol de Oliveira, B.; Storchi-Bergmann, T.; Morganti, R.; Riffel, R.A.; Ramakrishnan, V. Cold molecular gas outflow encasing the ionized one in the Seyfert galaxy NGC 3281. *Mon. Not. R. Astron. Soc.* **2023**, *522*, 3753–3765.
35. Gelderman, R.; Whittle, M. An Optical Study of Compact Steep-Spectrum Radio Sources. I. The Spectroscopic Data. *Astrophys. J. Suppl. Ser.* **1994**, *91*, 491. [CrossRef]
36. Labiano, A.; García-Burillo, S.; Combes, F.; Usero, A.; Soria-Ruiz, R.; Tremblay, G.; Neri, R.; Fuente, A.; Morganti, R.; Oosterloo, T. Fueling the central engine of radio galaxies. II. The footprints of AGN feedback on the ISM of 3C 236. *Astron. Astrophys.* **2013**, *549*, A58.

37. Mahony, E.K.; Oonk, J.B.R.; Morganti, R.; Tadhunter, C.; Bessiere, P.; Short, P.; Emonts, B.H.C.; Oosterloo, T.A. Jet-driven outflows of ionized gas in the nearby radio galaxy 3C 293. *Mon. Not. R. Astron. Soc.* **2016**, *455*, 2453–2460.
38. Woo, J.H.; Bae, H.J.; Son, D.; Karouzos, M. The Prevalence of Gas Outflows in Type 2 AGNs. *Astrophys. J.* **2016**, *817*, 108.
39. Jarvis, M.E.; Harrison, C.M.; Thomson, A.P.; Circosta, C.; Mainieri, V.; Alexander, D.M.; Edge, A.C.; Lansbury, G.B.; Molyneux, S.J.; Mullaney, J.R. Prevalence of radio jets associated with galactic outflows and feedback from quasars. *Mon. Not. R. Astron. Soc.* **2019**, *485*, 2710–2730.
40. Venturi, G.; Cresci, G.; Marconi, A.; Mingozzi, M.; Nardini, E.; Carniani, S.; Mannucci, F.; Marasco, A.; Maiolino, R.; Perna, M.; et al. MAGNUM survey: Compact jets causing large turmoil in galaxies. Enhanced line widths perpendicular to radio jets as tracers of jet-ISM interaction. *Astron. Astrophys.* **2021**, *648*, A17.
41. Zakamska, N.L.; Greene, J.E. Quasar feedback and the origin of radio emission in radio-quiet quasars. *Mon. Not. R. Astron. Soc.* **2014**, *442*, 784–804.
42. Zakamska, N.L.; Lampayan, K.; Petric, A.; Dicken, D.; Greene, J.E.; Heckman, T.M.; Hickox, R.C.; Ho, L.C.; Krolik, J.H.; Nesvadba, N.P.H.; et al. Star formation in quasar hosts and the origin of radio emission in radio-quiet quasars. *Mon. Not. R. Astron. Soc.* **2016**, *455*, 4191–4211.
43. Wylezalek, D.; Zakamska, N.L.; Liu, G.; Obied, G. Towards a comprehensive picture of powerful quasars, their host galaxies and quasar winds at z $\sim$ 0.5. *Mon. Not. R. Astron. Soc.* **2016**, *457*, 745–763.
44. Wylezalek, D.; Zakamska, N.L.; Greene, J.E.; Riffel, R.A.; Drory, N.; Andrews, B.H.; Merloni, A.; Thomas, D. SDSS-IV MaNGA: Identification of active galactic nuclei in optical integral field unit surveys. *Mon. Not. R. Astron. Soc.* **2018**, *474*, 1499–1514. [CrossRef]
45. Blundell, K.M.; Kuncic, Z. On the Origin of Radio Core Emission in Radio-quiet Quasars. *Astrophys. J.* **2007**, *668*, L103–L106.
46. Hwang, H.C.; Zakamska, N.L.; Alexandroff, R.M.; Hamann, F.; Greene, J.E.; Perrotta, S.; Richards, G.T. Winds as the origin of radio emission in z = 2.5 radio-quiet extremely red quasars. *Mon. Not. R. Astron. Soc.* **2018**, *477*, 830–844.
47. Kraemer, S.B.; Crenshaw, D.M.; Hutchings, J.B.; George, I.M.; Danks, A.C.; Gull, T.R.; Kaiser, M.E.; Nelson, C.H.; Weistrop, D.; Vieira, G.L. Space Telescope Imaging Spectrograph Echelle Observations of the Seyfert Galaxy NGC 4151: Physical Conditions in the Ultraviolet Absorbers. *Astrophys. J.* **2001**, *551*, 671–686.
48. Kraemer, S.B.; Tombesi, F.; Bottorff, M.C. Physical Conditions in Ultra-fast Outflows in AGN. *Astrophys. J.* **2018**, *852*, 35. [CrossRef]
49. Husemann, B.; Scharwächter, J.; Davis, T.A.; Pérez-Torres, M.; Smirnova-Pinchukova, I.; Tremblay, G.R.; Krumpe, M.; Combes, F.; Baum, S.A.; Busch, G.; et al. The Close AGN Reference Survey (CARS). A massive multi-phase outflow impacting the edge-on galaxy HE 1353-1917. *Astron. Astrophys.* **2019**, *627*, A53.
50. Girdhar, A.; Harrison, C.M.; Mainieri, V.; Bittner, A.; Costa, T.; Kharb, P.; Mukherjee, D.; Arrigoni Battaia, F.; Alexander, D.M.; Calistro Rivera, G.; et al. Quasar feedback survey: Multiphase outflows, turbulence, and evidence for feedback caused by low power radio jets inclined into the galaxy disc. *Mon. Not. R. Astron. Soc.* **2022**, *512*, 1608–1628.
51. Kellermann, K.I.; Sramek, R.; Schmidt, M.; Shaffer, D.B.; Green, R. VLA Observations of Objects in the Palomar Bright Quasar Survey. *Astron. J.* **1989**, *98*, 1195. [CrossRef]
52. Miller, L.; Peacock, J.A.; Mead, A.R.G. The bimodal radio luminosity function of quasars. *Mon. Not. R. Astron. Soc.* **1990**, *244*, 207–213.
53. Kellermann, K.I.; Condon, J.J.; Kimball, A.E.; Perley, R.A.; Ivezić, Ž. Radio-loud and Radio-quiet QSOs. *Astrophys. J.* **2016**, *831*, 168.
54. O'Dea, C.P.; Saikia, D.J. Compact steep-spectrum and peaked-spectrum radio sources. *Astron. Astrophys. Rev.* **2021**, *29*, 3.
55. Blandford, R.; Meier, D.; Readhead, A. Relativistic Jets from Active Galactic Nuclei. *Annu. Rev. Astron. Astrophys.* **2019**, *57*, 467–509.
56. Saikia, D.J. Jets in radio galaxies and quasars: An observational perspective. *J. Astrophys. Astron.* **2022**, *43*, 97.
57. Ulvestad, J.S.; Wrobel, J.M.; Roy, A.L.; Wilson, A.S.; Falcke, H.; Krichbaum, T.P. Subrelativistic Radio Jets and Parsec-Scale Absorption in Two Seyfert Galaxies. *Astrophys. J.* **1999**, *517*, L81–L84.
58. Lal, D.V.; Shastri, P.; Gabuzda, D.C. Seyfert Galaxies: Nuclear Radio Structure and Unification. *Astrophys. J.* **2011**, *731*, 68.
59. Panessa, F.; Baldi, R.D.; Laor, A.; Padovani, P.; Behar, E.; McHardy, I. The origin of radio emission from radio-quiet active galactic nuclei. *Nat. Astron.* **2019**, *3*, 387–396.
60. Padovani, P. On the two main classes of active galactic nuclei. *Nat. Astron.* **2017**, *1*, 0194.
61. Laing, R.A.; Bridle, A.H. Systematic properties of decelerating relativistic jets in low-luminosity radio galaxies. *Mon. Not. R. Astron. Soc.* **2014**, *437*, 3405–3441.
62. Mukherjee, D.; Bicknell, G.V.; Wagner, A.Y.; Sutherland, R.S.; Silk, J. Relativistic jet feedback—III. Feedback on gas discs. *Mon. Not. R. Astron. Soc.* **2018**, *479*, 5544–5566.
63. Massaglia, S.; Bodo, G.; Rossi, P.; Capetti, S.; Mignone, A. Making Faranoff-Riley I radio sources. II. The effects of jet magnetization. *Astron. Astrophys.* **2019**, *621*, A132.
64. Kharb, P.; Silpa, S. Looking for Signatures of AGN Feedback in Radio-Quiet AGN. *Galaxies* **2023**, *11*, 27.
65. Ulvestad, J.S.; Wilson, A.S. Radio structures of Seyfert galaxies. V. A flux-limited sample of Markarian galaxies. *Astrophys. J.* **1984**, *278*, 544–557. [CrossRef]
66. Ulvestad, J.S.; Wilson, A.S. Radio structures of Seyfert galaxies. VI. VLA observations of a nearby sample. *Astrophys. J.* **1984**, *285*, 439–452. [CrossRef]

67. Orienti, M.; Prieto, M.A. Radio structures of the nuclei of nearby Seyfert galaxies and the nature of the missing diffuse emission. *Mon. Not. R. Astron. Soc.* **2010**, *401*, 2599–2610.
68. Ulvestad, J.S.; Wilson, A.S. Radio Structures of Seyfert Galaxies. VII. Extension of a Distance-limited Sample. *Astrophys. J.* **1989**, *343*, 659. [CrossRef]
69. Miller, P.; Rawlings, S.; Saunders, R. The radio and optical properties of the Z < 0.5 BQS quasars. *Mon. Not. R. Astron. Soc.* **1993**, *263*, 425–460. [CrossRef]
70. Kukula, M.J.; Pedlar, A.; Baum, S.A.; O'Dea, C.P. High-resolution radio observations of the CfA Seyfert Sample -I. The observations. *Mon. Not. R. Astron. Soc.* **1995**, *276*, 1262–1280. [CrossRef]
71. Morganti, R.; Tsvetanov, Z.I.; Gallimore, J.; Allen, M.G. Radio continuum morphology of southern Seyfert galaxies. *Astron. Astrophys. Suppl. Ser.* **1999**, *137*, 457–471. [CrossRef]
72. Ulvestad, J.S.; Ho, L.C. Statistical Properties of Radio Emission from the Palomar Seyfert Galaxies. *Astrophys. J.* **2001**, *558*, 561–577.
73. Ho, L.C.; Ulvestad, J.S. Radio Continuum Survey of an Optically Selected Sample of Nearby Seyfert Galaxies. *Astrophys. J. Suppl. Ser.* **2001**, *133*, 77–118.
74. Thean, A.; Pedlar, A.; Kukula, M.J.; Baum, S.A.; O'Dea, C.P. High-resolution radio observations of Seyfert galaxies in the extended 12-μm sample—II. The properties of compact radio components. *Mon. Not. R. Astron. Soc.* **2001**, *325*, 737–760.
75. Thean, A.H.C.; Gillibrand, T.I.; Pedlar, A.; Kukula, M.J. MERLIN radio observations of CfA Seyferts. *Mon. Not. R. Astron. Soc.* **2001**, *327*, 369–384. [CrossRef]
76. Neff, S.G.; de Bruyn, A.G. The compact radio core of MKN 348: Evidence for directed outflow in a type 2 Seyfert galaxy. *Astron. Astrophys.* **1983**, *128*, 318–324.
77. Roy, A.L.; Norris, R.P.; Kesteven, M.J.; Troup, E.R.; Reynolds, J.E. Compact Radio Cores in Seyfert Galaxies. *Astrophys. J.* **1994**, *432*, 496.
78. Mundell, C.G.; Wilson, A.S.; Ulvestad, J.S.; Roy, A.L. Parsec-Scale Images of Flat-Spectrum Radio Sources in Seyfert Galaxies. *Astrophys. J.* **2000**, *529*, 816–831.
79. Nagar, N.M.; Falcke, H.; Wilson, A.S.; Ulvestad, J.S. Radio sources in low-luminosity active galactic nuclei. III. "AGNs" in a distance-limited sample of "LLAGNs". *Astron. Astrophys.* **2002**, *392*, 53–82. [CrossRef]
80. Ulvestad, J.S.; Wong, D.S.; Taylor, G.B.; Gallimore, J.F.; Mundell, C.G. VLBA Identification of the Milliarcsecond Active Nucleus in the Seyfert Galaxy NGC 4151. *Astron. J.* **2005**, *130*, 936–944.
81. Kukula, M.J.; Ghosh, T.; Pedlar, A.; Schilizzi, R.T. Parsec-Scale Radio Structures in the Nuclei of Four Seyfert Galaxies. *Astrophys. J.* **1999**, *518*, 117–128.
82. Mundell, C.G.; Wrobel, J.M.; Pedlar, A.; Gallimore, J.F. The Nuclear Regions of the Seyfert Galaxy NGC 4151: Parsec-Scale H I Absorption and a Remarkable Radio Jet. *Astrophys. J.* **2003**, *583*, 192–204.
83. Middelberg, E.; Roy, A.L.; Nagar, N.M.; Krichbaum, T.P.; Norris, R.P.; Wilson, A.S.; Falcke, H.; Colbert, E.J.M.; Witzel, A.; Fricke, K.J. Motion and properties of nuclear radio components in Seyfert galaxies seen with VLBI. *Astron. Astrophys.* **2004**, *417*, 925–944. [CrossRef]
84. Giroletti, M.; Panessa, F. The Faintest Seyfert Radio Cores Revealed by VLBI. *Astrophys. J.* **2009**, *706*, L260–L264.
85. Xanthopoulos, E.; Thean, A.H.C.; Pedlar, A.; Richards, A.M.S. Linear radio structures in selected Seyfert galaxies. *Mon. Not. R. Astron. Soc.* **2010**, *404*, 1966–1983. [CrossRef]
86. Gallimore, J.F.; Baum, S.A.; O'Dea, C.P.; Pedlar, A. The Subarcsecond Radio Structure in NGC 1068. I. Observations and Results. *Astrophys. J.* **1996**, *458*, 136. [CrossRef]
87. Williams, D.R.A.; McHardy, I.M.; Baldi, R.D.; Beswick, R.J.; Argo, M.K.; Dullo, B.T.; Knapen, J.H.; Brinks, E.; Fenech, D.M.; Mundell, C.G.; et al. Radio jets in NGC 4151: Where eMERLIN meets HST. *Mon. Not. R. Astron. Soc.* **2017**, *472*, 3842–3853.
88. Falle, S.A.E.G. Self-similar jets. *Mon. Not. R. Astron. Soc.* **1991**, *250*, 581–596. [CrossRef]
89. Begelman, M.C. Baby Cygnus A's. In *Cygnus A—Studay of a Radio Galaxy*; Carilli, C.L.; Harris, D.E., Eds.; Cambridge University Press: Cambridge, UK , 1996; p. 209.
90. Kaiser, C.R.; Alexander, P. A self-similar model for extragalactic radio sources. *Mon. Not. R. Astron. Soc.* **1997**, *286*, 215–222. [CrossRef]
91. Alexander, P. Evolutionary models for radio sources from compact sources to classical doubles. *Mon. Not. R. Astron. Soc.* **2000**, *319*, 8–16. [CrossRef]
92. Snellen, I.A.G.; Schilizzi, R.T.; van Langevelde, H.J. Multifrequency VLBI observations of faint gigahertz peaked spectrum sources. *Mon. Not. R. Astron. Soc.* **2000**, *319*, 429–444.
93. Carvalho, J.C.; O'Dea, C.P. Evolution of Global Properties of Powerful Radio Sources. I. Hydrodynamical Simulations in a Constant Density Atmosphere and Comparison with Self-similar Models. *Astrophys. J. Suppl. Ser.* **2002**, *141*, 337–370. [CrossRef]
94. Middelberg, E.; Agudo, I.; Roy, A.L.; Krichbaum, T.P. Jet-cloud collisions in the jet of the Seyfert galaxy NGC3079. *Mon. Not. R. Astron. Soc.* **2007**, *377*, 731–740.
95. Roy, A.L.; Wilson, A.S.; Ulvestad, J.S.; Colbert, J.M. Slow jets in Seyfert Galaxies: NGC1068. In Proceedings of the 5th European VLBI Network Symposium, Onsala, Sweden, 29 June–1 July 2000; Conway, J.E., Polatidis, A.G., Booth, R.S., Pihlström, Y.M., Eds.; Chalmers Technical University: Gothenburg, Sweden, 2000; p. 7.
96. Ulvestad, J.S.; Roy, A.L.; Colbert, E.J.M.; Wilson, A.S. A Subparsec Radio Jet or Disk in NGC 4151. *Astrophys. J.* **1998**, *496*, 196–202. [CrossRef]

97. Axon, D.J.; Marconi, A.; Capetti, A.; Macchetto, F.D.; Schreier, E.; Robinson, A. Jet-Driven Motions in the Narrow-Line Region of NGC 1068. *Astrophys. J.* **1998**, *496*, L75–L78. [CrossRef]
98. Bicknell, G.V.; Dopita, M.A.; Tsvetanov, Z.I.; Sutherland, R.S. Are Seyfert Narrow-Line Regions Powered by Radio Jets? *Astrophys. J.* **1998**, *495*, 680–690.
99. Capetti, A.; Macchetto, F.; Axon, D.J.; Sparks, W.B.; Boksenberg, A. The Morphology of the Narrow-Line Region of Markarian 3. *Astrophys. J.* **1995**, *448*, 600. [CrossRef]
100. Capetti, A.; Axon, D.J.; Macchetto, F.; Sparks, W.B.; Boksenberg, A. Radio Outflows and the Origin of the Narrow-Line Region in Seyfert Galaxies. *Astrophys. J.* **1996**, *469*, 554. [CrossRef]
101. Capetti, A.; Axon, D.J.; Macchetto, F.D.; Marconi, A.; Winge, C. The Origin of the Narrow-Line Region of Markarian 3: An Overpressured Jet Cocoon. *Astrophys. J.* **1999**, *516*, 187–194.
102. Crenshaw, D.M.; Kraemer, S.B. Resolved Spectroscopy of the Narrow-Line Region in NGC 1068: Kinematics of the Ionized Gas. *Astrophys. J.* **2000**, *532*, L101–L104.
103. García-Burillo, S.; Combes, F.; Usero, A.; Aalto, S.; Krips, M.; Viti, S.; Alonso-Herrero, A.; Hunt, L.K.; Schinnerer, E.; Baker, A.J.; et al. Molecular line emission in NGC 1068 imaged with ALMA. I. An AGN-driven outflow in the dense molecular gas. *Astron. Astrophys.* **2014**, *567*, A125.
104. Geballe, T.R.; Mason, R.E.; Oka, T. Outflowing Diffuse Gas in the Active Galactic Nucleus of NGC 1068. *Astrophys. J.* **2015**, *812*, 56.
105. Gallimore, J.F.; Elitzur, M.; Maiolino, R.; Marconi, A.; O'Dea, C.P.; Lutz, D.; Baum, S.A.; Nikutta, R.; Impellizzeri, C.M.V.; Davies, R.; et al. High-velocity Bipolar Molecular Emission from an AGN Torus. *Astrophys. J.* **2016**, *829*, L7.
106. May, D.; Steiner, J.E. A two-stage outflow in NGC 1068. *Mon. Not. R. Astron. Soc.* **2017**, *469*, 994–1025.
107. Impellizzeri, C.M.V.; Gallimore, J.F.; Baum, S.A.; Elitzur, M.; Davies, R.; Lutz, D.; Maiolino, R.; Marconi, A.; Nikutta, R.; O'Dea, C.P.; et al. Counter-rotation and High-velocity Outflow in the Parsec-scale Molecular Torus of NGC 1068. *Astrophys. J.* **2019**, *884*, L28.
108. Kinkhabwala, A.; Sako, M.; Behar, E.; Kahn, S.M.; Paerels, F.; Brinkman, A.C.; Kaastra, J.S.; Gu, M.F.; Liedahl, D.A. XMM-Newton Reflection Grating Spectrometer Observations of Discrete Soft X-ray Emission Features from NGC 1068. *Astrophys. J.* **2002**, *575*, 732–746.
109. Evans, D.A.; Ogle, P.M.; Marshall, H.L.; Nowak, M.A.; Bianchi, S.; Guainazzi, M.; Longinotti, A.L.; Dewey, D.; Schulz, N.S.; Noble, M.S.; et al. Searching for AGN Outflows: Spatially Resolved Chandra HETG Spectroscopy of the NLR Ionization Cone in NGC 1068. *arXiv* **2010**, arXiv.0910.3023.
110. Kallman, T.; Evans, D.A.; Marshall, H.; Canizares, C.; Longinotti, A.; Nowak, M.; Schulz, N. A Census of X-ray Gas in NGC 1068: Results from 450 ks of Chandra High Energy Transmission Grating Observations. *Astrophys. J.* **2014**, *780*, 121.
111. Kraemer, S.B.; Sharma, N.; Turner, T.J.; George, I.M.; Crenshaw, D.M. Physical Conditions in the X-ray Emission-line Gas in NGC 1068. *Astrophys. J.* **2015**, *798*, 53.
112. Hummel, E.; van Gorkom, J.H.; Kotanyi, C.G. Anomalous radio continuum features in edge-on spiral galaxies. *Astrophys. J.* **1983**, *267*, L5–L9. [CrossRef]
113. Stone, J.L., Jr.; Wilson, A.S.; Ward, M.J. Collimated Nuclear Ejection of Radio-Emitting Plasma in the Seyfert Galaxy NGC 4388. *Astrophys. J.* **1988**, *330*, 105. [CrossRef]
114. Baum, S.A.; O'Dea, C.P.; Dallacassa, D.; de Bruyn, A.G.; Pedlar, A. Kiloparsec-Scale Radio Emission in Seyfert Galaxies: Evidence for Starburst-driven Superwinds? *Astrophys. J.* **1993**, *419*, 553. [CrossRef]
115. Colbert, E.J.M.; Baum, S.A.; Gallimore, J.F.; O'Dea, C.P.; Christensen, J.A. Large-Scale Outflows in Edge-on Seyfert Galaxies. II. Kiloparsec-Scale Radio Continuum Emission. *Astrophys. J.* **1996**, *467*, 551.
116. Gallimore, J.F.; Axon, D.J.; O'Dea, C.P.; Baum, S.A.; Pedlar, A. A Survey of Kiloparsec-Scale Radio Outflows in Radio-Quiet Active Galactic Nuclei. *Astron. J.* **2006**, *132*, 546–569.
117. Singh, V.; Ishwara-Chandra, C.H.; Wadadekar, Y.; Beelen, A.; Kharb, P. Kiloparsec-scale radio emission in Seyfert and LINER galaxies. *Mon. Not. R. Astron. Soc.* **2015**, *446*, 599–612.
118. Smith, K.L.; Koss, M.; Mushotzky, R.; Wong, O.I.; Shimizu, T.T.; Ricci, C.; Ricci, F. Significant Suppression of Star Formation in Radio-quiet AGN Host Galaxies with Kiloparsec-scale Radio Structures. *Astrophys. J.* **2020**, *904*, 83.
119. Colbert, E.J.M.; Baum, S.A.; Gallimore, J.F.; O'Dea, C.P.; Lehnert, M.D.; Tsvetanov, Z.I.; Mulchaey, J.S.; Caganoff, S. Large-Scale Outflows in Edge-on Seyfert Galaxies. I. Optical Emission-Line Imaging and Optical Spectroscopy. *Astrophys. J. Suppl. Ser.* **1996**, *105*, 75.
120. Colbert, E.J.M.; Baum, S.A.; O'Dea, C.P.; Veilleux, S. Large-Scale Outflows in Edge-on Seyfert Galaxies. III. Kiloparsec-Scale Soft X-ray Emission. *Astrophys. J.* **1998**, *496*, 786–796. [CrossRef]
121. Sebastian, B.; Kharb, P.; O'Dea, C.P.; Gallimore, J.F.; Baum, S.A. A radio polarimetric study to disentangle AGN activity and star formation in Seyfert galaxies. *Mon. Not. R. Astron. Soc.* **2020**, *499*, 334–354.
122. Gaspari, M.; Brighenti, F.; Temi, P. Mechanical AGN feedback: Controlling the thermodynamical evolution of elliptical galaxies. *Mon. Not. R. Astron. Soc.* **2012**, *424*, 190–209.
123. Bourne, M.A.; Sijacki, D. AGN jet feedback on a moving mesh: Cocoon inflation, gas flows and turbulence. *Mon. Not. R. Astron. Soc.* **2017**, *472*, 4707–4735.
124. Villar-Martín, M.; Tadhunter, C.; Morganti, R.; Axon, D.; Koekemoer, A. PKS 2250-41 and the role of jet-cloud interactions in powerful radio galaxies. *Mon. Not. R. Astron. Soc.* **1999**, *307*, 24–40.

125. Mullaney, J.R.; Alexander, D.M.; Fine, S.; Goulding, A.D.; Harrison, C.M.; Hickox, R.C. Narrow-line region gas kinematics of 24 264 optically selected AGN: The radio connection. *Mon. Not. R. Astron. Soc.* **2013**, *433*, 622–638.
126. Heckman, T.M.; Miley, G.K.; van Breugel, W.J.M.; Butcher, H.R. Emission-line profiles and kinematics of the narrow-line region in Seyfert and radio galaxies. *Astrophys. J.* **1981**, *247*, 403–418. [CrossRef]
127. Whittle, M. Virial and Jet-induced Velocities in Seyfert Galaxies. II. Galaxy Rotation as Virial Parameter. *Astrophys. J.* **1992**, *387*, 109. [CrossRef]
128. Blundell, K.M.; Beasley, A.J. The central engines of radio-quiet quasars. *Mon. Not. R. Astron. Soc.* **1998**, *299*, 165–170.
129. Tadhunter, C.; Marconi, A.; Axon, D.; Wills, K.; Robinson, T.G.; Jackson, N. Spectroscopy of the near-nuclear regions of Cygnus A: Estimating the mass of the supermassive black hole. *Mon. Not. R. Astron. Soc.* **2003**, *342*, 861–875.
130. Holt, J.; Tadhunter, C.; Morganti, R.; Bellamy, M.; González Delgado, R.M.; Tzioumis, A.; Inskip, K.J. The co-evolution of the obscured quasar PKS 1549-79 and its host galaxy: Evidence for a high accretion rate and warm outflow. *Mon. Not. R. Astron. Soc.* **2006**, *370*, 1633–1650.
131. Holt, J.; Tadhunter, C.N.; Morganti, R. Fast outflows in compact radio sources: Evidence for AGN-induced feedback in the early stages of radio source evolution. *Mon. Not. R. Astron. Soc.* **2008**, *387*, 639–659.
132. Morganti, R.; Oosterloo, T.A.; Emonts, B.H.C.; van der Hulst, J.M.; Tadhunter, C.N. Fast Outflow of Neutral Hydrogen in the Radio Galaxy 3C 293. *Astrophys. J.* **2003**, *593*, L69–L72.
133. Morganti, R.; Tadhunter, C.N.; Oosterloo, T.A. Fast neutral outflows in powerful radio galaxies: A major source of feedback in massive galaxies. *Astron. Astrophys.* **2005**, *444*, L9–L13. [CrossRef]
134. Oosterloo, T.A.; Morganti, R.; Tzioumis, A.; Reynolds, J.; King, E.; McCulloch, P.; Tsvetanov, Z. A Strong Jet-Cloud Interaction in the Seyfert Galaxy IC 5063: VLBI Observations. *Astron. J.* **2000**, *119*, 2085–2091.
135. Alatalo, K.; Blitz, L.; Young, L.M.; Davis, T.A.; Bureau, M.; Lopez, L.A.; Cappellari, M.; Scott, N.; Shapiro, K.L.; Crocker, A.F.; et al. Discovery of an Active Galactic Nucleus Driven Molecular Outflow in the Local Early-type Galaxy NGC 1266. *Astrophys. J.* **2011**, *735*, 88.
136. Morganti, R.; Oosterloo, T.; Raymond Oonk, J.B.; Frieswijk, W.; Tadhunter, C. The fast molecular outflow in the Seyfert galaxy IC 5063 as seen by ALMA. *Astron. Astrophys.* **2015**, *580*, A1. [CrossRef]
137. Morganti, R.; Veilleux, S.; Oosterloo, T.; Teng, S.H.; Rupke, D. Another piece of the puzzle: The fast H I outflow in Mrk 231. *Astron. Astrophys.* **2016**, *593*, A30.
138. Cavagnolo, K.W.; McNamara, B.R.; Nulsen, P.E.J.; Carilli, C.L.; Jones, C.; Bîrzan, L. A Relationship Between AGN Jet Power and Radio Power. *Astrophys. J.* **2010**, *720*, 1066–1072.
139. Hopkins, P.F.; Elvis, M. Quasar feedback: More bang for your buck. *Mon. Not. R. Astron. Soc.* **2010**, *401*, 7–14.
140. Elmouttie, M.; Koribalski, B.; Gordon, S.; Taylor, K.; Houghton, S.; Lavezzi, T.; Haynes, R.; Jones, K. The kinematics of the ionized gas in the Circinus galaxy. *Mon. Not. R. Astron. Soc.* **1998**, *297*, 49–68. [CrossRef]
141. Cecil, G.; Bland-Hawthorn, J.; Veilleux, S.; Filippenko, A.V. Jet- and Wind-driven Ionized Outflows in the Superbubble and Star-forming Disk of NGC 3079. *Astrophys. J.* **2001**, *555*, 338–355.
142. Hota, A.; Saikia, D.J. Radio bubbles in the composite AGN-starburst galaxy NGC6764. *Mon. Not. R. Astron. Soc.* **2006**, *371*, 945–956.
143. Mingo, B.; Hardcastle, M.J.; Croston, J.H.; Evans, D.A.; Hota, A.; Kharb, P.; Kraft, R.P. Markarian 6: Shocking the Environment of an Intermediate Seyfert. *Astrophys. J.* **2011**, *731*, 21.
144. Alatalo, K.; Lacy, M.; Lanz, L.; Bitsakis, T.; Appleton, P.N.; Nyland, K.; Cales, S.L.; Chang, P.; Davis, T.A.; de Zeeuw, P.T.; et al. Suppression of Star Formation in NGC 1266. *Astrophys. J.* **2015**, *798*, 31.
145. Finlez, C.; Nagar, N.M.; Storchi-Bergmann, T.; Schnorr-Müller, A.; Riffel, R.A.; Lena, D.; Mundell, C.G.; Elvis, M.S. The complex jet- and bar-perturbed kinematics in NGC 3393 as revealed with ALMA and GEMINI-GMOS/IFU. *Mon. Not. R. Astron. Soc.* **2018**, *479*, 3892–3908.
146. King, A. The AGN-Starburst Connection, Galactic Superwinds, and M_{BH}-σ. *Astrophys. J.* **2005**, *635*, L121–L123.
147. Zubovas, K.; King, A. Clearing Out a Galaxy. *Astrophys. J.* **2012**, *745*, L34.
148. Perna, R.; Lazzati, D.; Cantiello, M. Electromagnetic Signatures of Relativistic Explosions in the Disks of Active Galactic Nuclei. *Astrophys. J.* **2021**, *906*, L7.
149. Liu, Y.; Wang, R.; Momjian, E.; Zhang, Y.; An, T.; Yang, X.; Wagg, J.; Bañados, E.; Omont, A. VLBA Reveals the Absence of a Compact Radio Core in the Radio-intermediate Quasar J2242+0334 at z = 5.9. *Astrophys. J. Lett.* **2022**, *939*, L5.
150. Liu, Y.; Wang, R.; Momjian, E.; Bañados, E.; Zeimann, G.; Willott, C.J.; Matsuoka, Y.; Omont, A.; Shao, Y.; Li, Q.; et al. Constraining the Quasar Radio-loud Fraction at z $\sim$ 6 with Deep Radio Observations. *Astrophys. J.* **2021**, *908*, 124.
151. Woo, J.H.; Son, D.; Bae, H.J. Delayed or No Feedback? Gas Outflows in Type 2 AGNs. III. *Astrophys. J.* **2017**. [CrossRef]
152. Rakshit, S.; Woo, J.H. A Census of Ionized Gas Outflows in Type 1 AGNs: Gas Outflows in AGNs. V. *Astrophys. J.* **2018**, *865*, 5.
153. Proga, D.; Stone, J.M.; Kallman, T.R. Dynamics of Line-driven Disk Winds in Active Galactic Nuclei. *Astrophys. J.* **2000**, *543*, 686–696.
154. Proga, D.; Kallman, T.R. Dynamics of Line-driven Disk Winds in Active Galactic Nuclei. II. Effects of Disk Radiation. *Astrophys. J.* **2004**, *616*, 688–695.
155. Begelman, M.C.; McKee, C.F.; Shields, G.A. Compton heated winds and coronae above accretion disks. I. Dynamics. *Astrophys. J.* **1983**, *271*, 70–88. [CrossRef]

156. Yuan, F.; Narayan, R. Hot Accretion Flows Around Black Holes. *Annu. Rev. Astron. Astrophys.* **2014**, *52*, 529–588.
157. Faucher-Giguère, C.A.; Quataert, E. The physics of galactic winds driven by active galactic nuclei. *Mon. Not. R. Astron. Soc.* **2012**, *425*, 605–622.
158. Husemann, B.; Singha, M.; Scharwächter, J.; McElroy, R.; Neumann, J.; Smirnova-Pinchukova, I.; Urrutia, T.; Baum, S.A.; Bennert, V.N.; Combes, F.; et al. The Close AGN Reference Survey (CARS). IFU survey data and the BH mass dependence of long-term AGN variability. *Astron. Astrophys.* **2022**, *659*, A124.
159. Singha, M.; Husemann, B.; Urrutia, T.; O'Dea, C.P.; Scharwächter, J.; Gaspari, M.; Combes, F.; Nevin, R.; Terrazas, B.A.; Pérez-Torres, M.; et al. The Close AGN Reference Survey (CARS). Locating the [O III] wing component in luminous local Type 1 AGN. *Astron. Astrophys.* **2022**, *659*, A123.
160. Winkel, N.; Husemann, B.; Singha, M.; Bennert, V.N.; Combes, F.; Davis, T.A.; Gaspari, M.; Jahnke, K.; McElroy, R.; O'Dea, C.P.; et al. The Close AGN Reference Survey (CARS). A parsec-scale multi-phase outflow in the super-Eddington NLS1 Mrk 1044. *Astron. Astrophys.* **2023**, *670*, A3.
161. Krongold, Y.; Longinotti, A.L.; Santos-Lleó, M.; Mathur, S.; Peterson, B.M.; Nicastro, F.; Gupta, A.; Rodríguez-Pascual, P.; Elías-Chávez, M. Detection of a Multiphase Ultrafast Wind in the Narrow-line Seyfert 1 Galaxy Mrk 1044. *Astrophys. J.* **2021**, *917*, 39.
162. Netzer, H. *The Physics and Evolution of Active Galactic Nuclei*; Cambridge University Press: Cambridge, UK, 2013. [CrossRef]
163. Longinotti, A.L.; Vega, O.; Krongold, Y.; Aretxaga, I.; Yun, M.; Chavushyan, V.; Feruglio, C.; Gómez-Ruiz, A.; Montaña, A.; León-Tavares, J.; et al. Early Science with the Large Millimeter Telescope: An Energy-driven Wind Revealed by Massive Molecular and Fast X-ray Outflows in the Seyfert Galaxy IRAS 17020+4544. *Astrophys. J. Lett.* **2018**, *867*, L11.
164. Liu, G.; Zakamska, N.L.; Greene, J.E.; Nesvadba, N.P.H.; Liu, X. Observations of feedback from radio-quiet quasars—I. Extents and morphologies of ionized gas nebulae. *Mon. Not. R. Astron. Soc.* **2013**, *430*, 2327–2345.
165. Schroetter, I.; Bouché, N.; Wendt, M.; Contini, T.; Finley, H.; Pelló, R.; Bacon, R.; Cantalupo, S.; Marino, R.A.; Richard, J.; et al. Muse Gas Flow and Wind (MEGAFLOW). I. First MUSE Results on Background Quasars. *Astrophys. J.* **2016**, *833*, 39.
166. Husemann, B.; Tremblay, G.; Davis, T.; Busch, G.; McElroy, R.; Neumann, J.; Urrutia, T.; Krumpe, M.; Scharwächter, J.; Powell, M.; et al. The Close AGN Reference Survey (CARS). *Messenger* **2017**, *169*, 42–47. [CrossRef]
167. McElroy, R.; Singha, M.; Husemann, B.; Davis, T.A.; Combes, F.; Scharwächter, J.; Smirnova-Pinchukova, I.; Pérez Torres, M.; Gaspari, M.; Winkel, N.; et al. The Close AGN Reference Survey (CARS): Data Release 1 and Beyond. *Messenger* **2022**, *187*, 3–7. [CrossRef]
168. Jakobsen, P.; Ferruit, P.; Alves de Oliveira, C.; Arribas, S.; Bagnasco, G.; Barho, R.; Beck, T.L.; Birkmann, S.; Böker, T.; Bunker, A.J.; et al. The Near-Infrared Spectrograph (NIRSpec) on the James Webb Space Telescope. I. Overview of the instrument and its capabilities. *Astron. Astrophys.* **2022**, *661*, A80.
169. Cresci, G.; Tozzi, G.; Perna, M.; Brusa, M.; Marconcini, C.; Marconi, A.; Carniani, S.; Brienza, M.; Giroletti, M.; Belfiore, F.; et al. Bubbles and outflows: The novel JWST/NIRSpec view of the z = 1.59 obscured quasar XID2028. *Astron. Astrophys.* **2023**, *672*, A128.
170. Veilleux, S.; Shopbell, P.L.; Miller, S.T. The Biconical Outflow in the Seyfert Galaxy NGC 2992. *Astron. J.* **2001**, *121*, 198–209.
171. Fischer, T.C.; Crenshaw, D.M.; Kraemer, S.B.; Schmitt, H.R.; Trippe, M.L. Modeling the Outflow in the Narrow-line Region of Markarian 573: Biconical Illumination of a Gaseous Disk. *Astron. J.* **2010**, *140*, 577–583.
172. Krieger, N.; Bolatto, A.D.; Walter, F.; Leroy, A.K.; Zschaechner, L.K.; Meier, D.S.; Ott, J.; Weiss, A.; Mills, E.A.C.; Levy, R.C.; et al. The Molecular Outflow in NGC 253 at a Resolution of Two Parsecs. *Astrophys. J.* **2019**, *881*, 43.
173. Shin, J.; Woo, J.H.; Chung, A.; Baek, J.; Cho, K.; Kang, D.; Bae, H.J. Positive and Negative Feedback of AGN Outflows in NGC 5728. *Astrophys. J.* **2019**, *881*, 147.
174. Perna, M.; Brusa, M.; Salvato, M.; Cresci, G.; Lanzuisi, G.; Berta, S.; Delvecchio, I.; Fiore, F.; Lutz, D.; Le Floc'h, E.; et al. SINFONI spectra of heavily obscured AGNs in COSMOS: Evidence of outflows in a MIR/O target at z $\sim$ 2.5. *Astron. Astrophys.* **2015**, *583*, A72.
175. Vardoulaki, E.; Jiménez Andrade, E.F.; Karim, A.; Novak, M.; Leslie, S.K.; Tisanić, K.; Smolčić, V.; Schinnerer, E.; Sargent, M.T.; Bondi, M.; et al. A closer look at the deep radio sky: Multi-component radio sources at 3 GHz VLA-COSMOS. *Astron. Astrophys.* **2019**, *627*, A142.
176. Gaibler, V.; Khochfar, S.; Krause, M.; Silk, J. Jet-induced star formation in gas-rich galaxies. *Mon. Not. R. Astron. Soc.* **2012**, *425*, 438–449.
177. Veilleux, S.; Liu, W.; Vayner, A.; Wylezalek, D.; Rupke, D.S.N.; Zakamska, N.L.; Ishikawa, Y.; Bertemes, C.; Barrera-Ballesteros, J.K.; Chen, H.W.; et al. First results from the JWST Early Release Science Program Q3D: The Warm Ionized Gas Outflow in z $\sim$ 1.6 Quasar XID 2028 and its Impact on the Host Galaxy. *arXiv* **2023**, arXiv:2303.08952. [CrossRef].